Utah State University

DigitalCommons@USU

All Graduate Theses and Dissertations

Graduate Studies

5-2015

Development of Genetic Goat and Hamster Models of Atrial Fibrillation and Long QT Syndrome; and Genetic Hamster Models of Middle East Respiratory Syndrome

Dane A. Rasmussen
Utah State University

Follow this and additional works at: https://digitalcommons.usu.edu/etd

Part of the Animal Sciences Commons, Genetics Commons, and the Molecular Biology Commons

Recommended Citation

UtahStateUniversity
MERRILL-CAZIER LIBRARY

DEVELOPMENT OF GENETIC GOAT AND HAMSTER MODELS OF ATRIAL

FIBRILLATION AND LONG QT SYNDROME; AND GENETIC HAMSTER

MODELS OF MIDDLE EAST RESPIRATORY SYNDROME

by

Dane A. Rasmussen

A thesis submitted in partial fulfillment
of the requirements for the degree

of

MASTER OF SCIENCE

in

Animal Molecular Genetics

Approved:

_____   _____
Zhongde Wang   S. Clay Isom
Major Professor   Committee Member

_____   _____
Brian Gowen   Mark McLellan
Committee Member   Vice President for Research and
                                         Dean of the School of Graduate Studies

UTAH STATE UNIVERSITY
Logan, Utah

2015

ABSTRACT

Development of Genetic Goat and Hamster Models of Atrial Fibrillation and Long QT

Syndrome; and Genetic Hamster Models of Middle East Respiratory Syndrome

by

Dane A. Rasmussen, Master of Science

Utah State University, 2015

Major Professor: Dr. Zhongde Wang
Department: Animal, Dairy and Veterinary Science

Atrial fibrillation, long QT syndrome, and Middle East Respiratory Syndrome are three

deadly human diseases for which genetic animal models are needed. From elucidating disease

pathogenesis to facilitating the development of treatments, animal models are crucial for studying

human disease. One of the most effective ways to generate specific animal models is through

genetic modification. Historically, mice have been most widely used as genetically modified

models, despite a number of limitations. New gene editing technologies such as CRISPR/Cas9

have made developing alternative genetic models that better recapitulate some human diseases

better and more feasible. In this thesis, I describe my efforts to develop genetically modified goat

and hamster models for atrial fibrillation and long QT syndrome, and genetically modified

hamster models for Middle East Respiratory Syndrome. For long QT syndrome model

development, I knocked out the *KCNQ1* gene in goat fetal fibroblast cells and baby hamster

kidney cells using the CRIPSR/Cas9 system. The knockout results in loss-of-function mutations,

a known cause of human long QT syndrome. The edited goat fibroblast cells will be nuclear

donors for future cloning experiments to produce live goats possessing the *KCNQ1* knockout. The

CRISPR gene targeting sgRNA/Cas9 vector, specific for the hamster *KCNQ1,* has been used for pronuclear injections to produce *KCNQ1* knockout hamsters. For atrial fibrillation model development, I designed a single-stranded donor oligonucleotide that generates a *KCNQ1* gain-of-function mutation resulting in the disease. This oligonucleotide was injected into hamster embryos along with the *KCNQ1* sgRNA/Cas9-expressing vector to generate hamsters containing the gain-of-function mutation. Finally, for Middle East Respiratory Syndrome model development, I established a breeding colony of human DPP4 transgenic hamsters in the *STAT2* knockout background. Human DPP4 transgenic hamsters are susceptible to MERS-CoV infection, showing mild clinical signs and allowing viral replication in lung tissue. Giving these hamsters a *STAT2* knockout background should promote a more severe disease progression. For all three diseases, the foundations for the development of genetic animal models have been laid.

(81 pages)

PUBLIC ABSTRACT

Development of Genetic Goat and Hamster Models of Atrial Fibrillation and Long QT
Syndrome; and Genetic Hamster Models of Middle East Respiratory Syndrome

Dane Rasmussen

Atrial fibrillation (AF) and long QT syndrome (LQTS) are potentially lethal heart rhythm disorders that can be caused by mutations in the potassium channel gene *KCNQ1*. Middle East Respiratory Syndrome (MERS) is a viral infection with the potential to replicate the devastating effects of the SARS outbreak in 2003. All three of these diseases are in need of genetic animal models.

To address these needs, my thesis project focused on the development of genetic goat and hamster models of AF and LQTS, and genetic hamster models of MERS. Because of the goat's similar organ size/physiology and the hamster's similar lipid metabolism to that of humans, we believe that these animals will make better models of these diseases than more common animals.

Utilizing the gene-editing technology CRISPR/Cas9, I knocked out the *KCNQ1* gene leading to a loss-of-function mutation known to cause LQTS, in goat and hamster cells. I also introduced a *KCNQ1* gain-of-function mutation, known to cause AF, into hamster cells. These *KCNQ1*-edited cells are currently being used to develop animals susceptible to AF and/or LQTS for these heart diseases.

I also developed a DPP4 transgenic hamster in a *STAT2* knockout background. The DPP4 transgene, encoding the human cell receptor for MERS virus entry, makes hamsters susceptible to MERS infection. The *STAT2* knockout may increase disease severity, more closely mimicking the human disease. These hamsters may be ideal animal models for MERS. The models developed from this work will be used to develop life-saving treatments for these three diseases.

ACKNOWLEDGMENTS

CONTENTS

LIST OF TABLES

LIST OF FIGURES

CHAPTER I

INTRODUCTION

Utility and Importance of Animal Models

Animal models are a key aspect in the study of virtually any disease [1]. Their utility can range from simply observing disease pathology to treatment testing. Testing novel treatments on animals first allows us to avoid the ethical concerns of testing potentially harmful substances on humans [2]. When human clinical drug trials are unethical or not feasible, the FDA will use data from an animal model when approving a new drug or vaccine. This is referred to as "The Animal Rule" [2, 3].

In some situations, wild type animals can be directly used as models for the study of certain human diseases. This was the case in using the nine banded armadillo (*Dasypus novemcinctus*) to model leprosy. Besides humans, the armadillo is the only organism susceptible to this disease, and the armadillo leprosy disease model has a disease progression similar to humans. Armadillos develop neurological involvement with *M. leprae*, the bacterial species that causes leprosy, which allows researchers to model the neuropathogenesis of leprosy. For these reasons, the armadillo has been the standard leprosy model for over forty years [4, 5].

Unfortunately, not all human diseases have a readily available wild type animal model. Because of this, the ability to generate specific genetic changes is essential for most animal model development. By altering the genetics of animals, disease susceptibility or resistance can be induced by inserting transgenes, altering a gene, or knocking out a gene's function entirely. Genetically engineered mouse models (GEMM's) have been extensively used to study a wide variety of diseases including cancer and neurodegenerative diseases [6-8]. Other genetic modifying techniques allow for increased control over gene expression. Tissue-specific and

temporal gene knockouts have been made possible by techniques such as the Cre-*lox*P

recombination, and tetracycline- or tamoxifen-induced systems [1, 9].

After initial use in mice, genetic modification technologies have extended to other

animals such as rats, hamsters, goats, pigs, cattle, sheep, and non-human primates [1]. It is worth

noting that site-specific genetic modifications were still impossible for some of these species,

such as hamsters and non-human primates. Although the mouse continues to be a powerhouse

model, the translatability to human conditions can sometimes be questionable. For example,

preclinical cancer drugs, usually tested in mouse models, have a poor track record in clinical trials

[10, 11]. Even though these drugs show promise in mouse models, the response rates to these

drugs are only 3.8% in patients [11].

The capability to develop genetically modified models in non-murine species has

improved human disease modeling, especially for the human diseases that cannot be adequately

modeled by mouse models. Take artherosclerosis for example. Mouse models have been widely

used for this disease, but lack key human lipid metabolism proteins [12]. Their coronary arteries,

the typical site of human artherosclerosis, are also too small to be investigated [13]. Pig models

have a similarly sized coronary artery to humans, allowing for mechanistic insights that could not

be previously investigated with mice [13]. Hamsters have provided another alternative

artherosclerosis model. Their lipid metabolism is more similar to humans, making them a better

model to study certain proteins involved in the artherosclerosis disease pattern [12].

This thesis focuses on the development of genetically engineered animal models for three

deadly human diseases: atrial fibrillation, long qt syndrome, and Middle East respiratory

syndrome. Both large animal and mouse models have been previously developed for atrial

fibrillation and long qt syndrome, but most current models do not address the role genetics play in

these diseases. There are some genetically modified mice of these diseases, but they are severely

limited by their small heart size and dissimilar physiology compared to humans. Making a large

genetic animal of these heart conditions, such as a goat, would address this limitation. An alternative small model with a more similar physiology to humans may also prove more useful than mice.

Recent efforts have led to some promising models for MERS. These models have demonstrated infectivity and have developed the disease, but so far it is unclear if they can be used for drug and vaccine testing. Additionally, developing another reliable model would likely improve our understanding of the disease, and would also potentially allow for the testing of MERS drugs and vaccines.

Due to the recent development of efficient genome editing technologies, the focus of my thesis was on using the CRISPR/Cas9 genome editing technology to generate these new animal models.

Heart Diseases to Be Modeled

Atrial Fibrillation

Atrial fibrillation (AF) is one the most common cardiac rhythm disorders seen in U.S. clinics [13]. It is a cardiac rhythm disorder characterized by "irregular and rapid electrical activity" in the atria [14]. Affecting mostly older people over 55, symptoms of AF include heart palpitations, fatigue, lightheadedness, and labored breathing [13]. There are also cases where AF occurs without presentation of apparent AF symptoms or other disease. This is referred to as Lone AF, and is more prevalent in younger patients [15]. Typically the irregular electrical activity progresses from paroxysmal, to persistent to permanent [16]. This progression can partially occur because of electrical and structural remodeling that occurs in the atria shortly after the first incidence of AF. This remodeling increases the likelihood of subsequent incidences of AF. Shortly put, "atrial fibrillation begets atrial fibrillation" [16-18].

Atrial Fibrillation has many risk factors including age. The risk of developing AF significantly increases after age 60, and this risk doubles with each decade of age [13]. AF is also more prevalent in males than in females [13]. Genetics is also a major risk factor for AF. When a parent has AF, the chance of their offspring also developing AF increases 2-3 fold [13]. Inherited atrial fibrillation is often referred to as "Familial AF" [15]. Like lone AF, familial AF seems to manifest itself at younger ages. Mutations of various ion channel genes have been observed in families with a history of AF [13, 15, 19]. One of the most commonly mutated genes leading to AF is the *KCNQ1* gene, which will be discussed later.

Atrial fibrillation is very prevalent in the United States. In 2009 about 2.3 million people were affected, and this number is expected to grow to 5.6 million by 2050 [13]. Originally thought to be benign in the absence of other heart conditions, AF has been found to be deadly on its own. In the absence of co-morbidity factors, AF was associated with nearly a two-fold increase in mortality from non-natural causes [20]. Additionally, AF can exacerbate other cardiac conditions and can increase the odds of their development.

One of the biggest concerns with AF is an increased incidence of ischemic strokes. About 75,000-100,000 strokes per year can be attributed to AF [13]. It is the most significant risk factor among all studied cardiac conditions, associated with a five-fold increase in the risk of developing a stroke compared to patients without AF [21]. Atrial fibrillation is also associated with congestive heart failure (CHF) [22]. Patients with AF have an increased risk of developing subsequent CHF. Likewise, patients with CHF have an increased risk of developing AF [13, 22].

The financial burden of AF can be staggering as well. In the United States the direct cost of AF in 2005 was estimated to be 6.65 billion USD. The cost of hospital visits alone was 2.93 billion USD where AF was the primary diagnosis [23]. Other countries have noticed a significant financial impact caused by AF as well. In 2000 the total estimated direct cost of AF in the UK was 459 million pounds, about 356 million USD during that year. [24].

Long QT Syndrome

Long QT syndrome (LQTS) is a cardiac arrhythmia characterized by a lengthened depolarization and repolarization phase of the cardiac action potential, or QT interval. Considered a relatively rare condition, LQTS is estimated to occur in between 1:2000 and 1:2500 births [25-26]. Left untreated, these episodes of lengthened QT intervals lead to syncope, seizures, and sudden cardiac death (SCD) [25]. There are two major variants of LQTS, Jervell & Lange-Nielsen syndrome and Romano-Ward syndrome. Both conditions cause lengthened QT intervals, and can lead to SCD. However, there are subtle differences in their clinical presentations, among which are that Jervell Lange-Nielsen syndrome is characterized by deafness, while Romano-Ward syndrome does not include deafness as a symptom [25].

There is a strong relationship between genotype and phenotype in LQTS patients. Currently LQTS is organized into 13 categories, designated LQT1 through LQT13. Each category of disease is caused by a mutation in a different gene [27]. The three most common forms of LQTS are LQT1, LQT2, and LQT3, caused by mutations in the *KCNQ1*, *KCNH2*, and *SCN5A* genes, respectively [26-27]. About 75% of all LQTS cases are caused by mutations in one of these three genes [26].

Age and gender factors are known to influence LQTS-associated SCD. Fatal cardiac events occur more frequently in children, particularly in preadolescence for boys and in adolescence and later for girls [28]. Zareba et al. reported that boys with LQT1, one of the most prevalent categories of LQTS, have a 71% higher risk of a cardiac event than girls [29]. SCD in LQT1 individuals is most often triggered during stressful or exertional situations such as swimming or emotional disturbances, but may also occur during rest [25]. LQTS can also be induced by certain medications, such as β-adrenergic agonists [30]. These factors can complicate LQTS diagnosis [25].

Genetics of AF and LQTS:
The *KCNQ1* Gene

As discussed briefly above, genetics is a key risk factor for both AF and LQTS. Genotype can greatly increase the likelihood of developing AF, especially in the cases of familial and lone AF [13, 15]. Although stress and medication help trigger syncope episodes from long QT syndrome, genetics is the main predisposing factor [25]. There are three major genes that contribute to LQTS susceptibility [25-27]. One of the most extensively studied genes associated with AF and LQTS is the potassium channel, voltage-gated KQT-like subfamily Q, member 1 (*KCNQ1*) gene. *KCNQ1* has been implicated in over 240 mutations causing AF, LQTS (specifically LQT1), and other heart conditions [31].

KCNQ1 codes for a voltage-gated potassium channel subunit found in many tissues such as heart, brain, and kidney [31]. The *KCNQ1* subunit consists of six transmembrane domains (S1-S6) [31]. The S1-S4 domains make up the voltage-sensing domain (VSD). This domain is responsible for detecting changes in membrane potential leading to a change in channel structure. The S5 and S6 domains form a pore region, where potassium ions are selectively allowed to flow in or out of the cell [31-32]. These subunits form a tetrameric pore-forming α-subunit. The architecture of this subunit is consistent with other voltage-gated potassium channels [32]. In heart tissue, the α-subunit combines with an auxiliary β-subunit, such as *KCNE1*; to form specialized voltage gated potassium channels. These specialized channels help form the current known as the slow delayed rectifier potassium current, which plays a major role in cardiac action potential repolarization [33]. In response to depolarization, the voltage-sensing domains change their structure, causing the pore region to open. This action allows potassium ions out of the cell. Once the cell membrane repolarizes, the VSD swings the pore region shut, halting potassium flow until the next depolarization [34].

Gain-of-function mutations have been associated with atrial fibrillation. For the last twelve years, a wide variety of *KCNQ1* gain-of-function mutations have been discovered. Two of the earliest mutations discovered, S140G and V141M, were point mutations located in S1 of the VSD [35-36]. Patch-clamping studies determined that these mutations slow channel inactivation when expressed with *KCNE1* in Xenopus oocytes [37]. After these studies, another point mutation, Q147R, was discovered. Similar patch-clamping studies found that this mutation could result in either an AF-like gain-of-function mutation or a loss-of-function mutation, depending on which β-subunit was co-expressed with the mutated gene [38].

Conversely, loss-of-function mutations at *KCNQ1* can be associated with LQTS, specifically LQT1 [31, 39-40]. *KCNQ1* mutations account for 40-55% of all cases of LQTS [27]. Mutation of one allele usually results in the development Romano-Ward syndrome. Biallelic mutations result in the more severe Jervell & Lange-Nielsen syndrome [25]. The different disease presentations between monoallelic and biallelic mutations in *KCNQ1* is consistent with the fact that *KCNQ1* is tissue-specifically imprinted. As *KCNQ1* is not imprinted in cardiac muscle, mutations on either alleles, depending on gain of function or loss of function mutations, should result in disease phenotypes (AF or LQTS) [41]. The types of *KCNQ1* loss-of-function mutations vary. While most of these mutations are single base pair substitutions or small insertions/deletions, there have been instances large deletions, duplications, and splicing mutations [26]. Novel *KCNQ1* mutations are still being uncovered [42].

The genetic knowledge of both AF and LQTS builds a bridge between molecular biology and clinical cardiology. Genetically modified animal models have played a critical role in establishing the current understanding of LQTS genetics. Yet, due to the significant limitations of the currently available animal models (discussed below), the ability to leverage this genetic knowledge into effective treatments and management strategies for these diseases is lacking. Because of the importance of *KCNQ1* to both AF and LQTS development, part of my project

focused on modifying *KCNQ1* in suitable animals to improve upon current models for these diseases.

Current Animal Models for AF and LQTS

Current Models of AF

In order to better understand the connections between genetics and disease symptoms of atrial fibrillation, developing animal models is vital. A wide variety of both small and large animal models have been developed previously for AF including: goats, dogs, pigs, sheep, rabbits, and mice [43]. Many techniques have been used to create these models. Large animal models have been primarily generated by surgical means, while mouse models have largely been produced through genetic techniques.

One of the first surgically induced large animal AF models was the sterile pericarditis dog model [43-44]. Sterile pericarditis, or surgical enlargement of the atria, was achieved by placement of wire electrodes on select areas of the atria. Using these animals, researchers could induce both AF and atrial flutter, a similar atrial arrhythmia [44].

Wijffels *et al* produced a goat model by surgical implantation of silicon strips containing electrodes on the atrial walls. With these implants, AF could be induced in these goats electronically by rapid atrial pacing [18, 45]. Sustained stimulation in this manner dangerously lowered atrial refractory periods in these goats [18]. This model contributed to the understanding that an episode of AF greatly increases the chances of additional AF episodes, and the phrase, "atrial fibrillation begets atrial fibrillation" was coined [18]. This conclusion has since been confirmed in dogs, sheep, and pigs [45].

Another dog model was made using similar surgical techniques i.e. surgical implantation of a pacemaker [46]. Studies using this model examined the effect of inducing AF on healthy

dogs compared to dogs with congestive heart failure (CHF), which has been previously associated with AF [22]. Atrial fibrillation was maintained in a greater number of CHF dogs than healthy dogs after electrical stimulation, further confirming the connection between CHF and AF [46].

In the above large animal models, atrial fibrillation is induced by electrical stimulation of the atria via surgically implanted pacemaker electrodes. Other manual surgical techniques have been utilized to induce AF including atrial volume overload, mitral regurgitation, and aortopulmonary shunts [43]. Since these models use surgical techniques that alter heart structure, they do not reliably present with a disease progression caused by genetic mutations. Additionally, these surgeries can be expensive and labor intensive. For these reasons there is a need for genetic animal models of atrial fibrillation.

Using a genetic manipulation approach, Marx *et al* produced a transgenic mouse expressing a h*KCNQ1*-h*KCNE1* fusion protein under the control of an α-myosin heavy chain promoter, which is expressed exclusively in cardiac tissue [47]. Although this group did not use this model to investigate AF directly, Sampson *et al* were able to produce AF-like arrhythmias in these mice [48]. Administration of isoprenaline, a β-adrenergic agonist, followed by atrial electrical stimulation induced prolonged atrial arrhythmias in these mice [48]. In another mouse genetic model, the mouse *KCNE1* gene was knocked out [49]. In these mice, spontaneous episodes of AF occurred in all *KCNE1* KO mice [50].

In addition to ion channel knockout models, other mechanisms have been used to generate AF models. Various connexin knockout mouse models have been used with varying success [51]. Overexpression of various genes to induce predisposing conditions of AF has also been used extensively [17]. For example, a mouse TGF-β_1 overexpression model was created to induce atrial fibrosis, a condition suspected to be a risk factor for AF [52]. Subsequent studies

with this model demonstrated an association between atrial fibrosis and an increased risk of AF [52].

Mouse models, though useful for studying some genetic causes of AF, have major limitations as AF models. Their heart size is considerably smaller than humans [53], and their cardiac channel physiology makes translating results from mouse studies to the human disease difficult. For example, the I_{KS} current in mice is not a main repolarizing current as it is in humans [48, 54]. This may be the reason why the severity of the AF phenotype is low in these models.

Many of the models mentioned above have contributed greatly to our understanding of the disease. However, there are questions about AF that current models are not suited to answer. Currently there are no genetically engineered large animal models available [43, 45]. As mentioned above, most large animal models were made by electric stimulation of surgically implanted electrodes. These procedures can be very invasive, and labor intensive. Having a genetically modified large animal model would be advantageous because model generation would be less invasive, and would allow us to do genotype-phenotype studies in animals with organ sizes and physiology more similar to that of humans.

Current Models for Long QT Syndrome

There have also been efforts towards generating long QT syndrome models. Rabbit, dog, and guinea pig hearts have been used as platforms to test drugs' potential to induce LQTS and associated arrhythmias such as Torsade de Pointes. In these models, ventricular wedges or whole hearts are isolated and perfused, treated with a candidate drug, and the resulting EKG's are examined for prolonged QT intervals, or other arrhythmias [55-57]. A dog atrioventricular block model was also made, and was also used to assess drug potentials' to induce LQTS [58]. These types of models have greatly helped our understanding of the disease. However these models are severely limited in that they can only be used to model drug-induced LQTS. Additionally, the

techniques mentioned above require either heart isolation resulting in animal sacrifice, or invasive surgical techniques to produce the model.

Much effort has been made into developing genetic mouse models of LQTS [54]. Of particular interest are the two *KCNQ1* KO models. Lee *et al* interrupted exon 1 of *KCNQ1* through insertion of a neomycin gene [59]. The resulting F2 and F3 animals showed no increase in QT interval, but mice homozygous for the interruption did display deafness, a key symptom of Jervell and Lange-Nielsen syndrome [59]. Another genetic mouse model was created by interrupting *KCNQ1* exon 2 through the insertion of a PKG-*neomycin* fusion cassette. Deafness manifested in all targeted animals, and prolonged QT intervals were observed in vivo but not in isolated hearts [60]. There is also a naturally occurring genetic mouse model for LQTS, the vertigo 2 Jackson mouse line that contains a spontaneous *KCNQ1* mutation. These mice are deaf, with gastric defects, and have a prolonged QT interval. However, there are no reports of SCD or any other severe LQTS clinical manifestations resulting from this spontaneous mutation [61].

The above examples highlight the limitations of mouse models in recapitulating SCD associated with LQTS. As analyzed by Nerbonne [53], the physiology of the mouse and human hearts differ. For example, the average human heart beats at 60-70 beats per minute, while the mouse heart beats about 10 times faster [53]. The driving forces of repolarization in the human and mouse hearts are also different, occurring through the delayed rectifier currents in humans but through transient outward currents in mice [48, 54]. Mouse cardiac action potentials and surface electrocardiograms also exhibit major differences from those of the human heart. Another sharp contrast between human and mouse hearts is anatomical: the size and overall shape of these hearts is vastly different [62].

To address some of the limitations of these mouse models, alternative models, such as rabbits have been explored. In rabbits, the advantages include the structural similarity of rabbit and human hearts [66], and similarities in electrophysiology, including the same potassium

current-based system for repolarization of the action potentials [63]. To exploit these strengths,

a rabbit model for LQT1 was developed in which the mutation that affects channel pore function

in human *KCNQ1* (KvLQT1-Y315S) was expressed in the rabbit heart under control of the rabbit

β-myosin heavy chain promoter [64]. This mutation prolonged the QT interval in rabbits similarly

to what occurs in LQT1 human patients. However, as in the mouse model, SCD was not observed

[64].

Middle East Respiratory Syndrome

Prevalence and Manifestations

MERS is an upper respiratory infection caused by the *Betacoronavirus* MERS-CoV [65-

67]. This disease has been shown to be especially dangerous to the elderly and the

immunocompromised [66-67]. Less commonly, MERS infects children, especially those with

underlying medical conditions [67-68]. Since November 11, 2015, there have been 1,611

laboratory-confirmed cases worldwide, with 575 confirmed deaths [69]. The clinical presentation

varies widely among individuals, ranging from an asymptomatic infection to fatal pneumonia

[67]. The common symptoms of MERS include: fever, cough, sore throat, headache, nausea,

vomiting, abdominal pain, diarrhea, muscle pain, and occasionally renal failure [66-67]. The

mode of transmission is not completely understood, but direct contact with infected individuals

and/or camels may be the predominant route [67]. Viral spread seems to be more efficient in

nosocomial settings, making hospital patients and healthcare workers especially vulnerable to

infection [67].

Genetically, MERS-CoV is most similar to a variety of bat coronaviruses including

HKU4 and HKU5 [66]. The dromedary camel is suspected to be the intermediate host of the virus,

though it is unclear if they are capable of virus transmission to humans [66]. MERS-CoV is very

similar to the coronavirus SARS-CoV, responsible for the SARS scare that occurred in 2003. SARS has similar clinical presentations to MERS, including severe respiratory tract disease and pneumonia [69]. During the SARS epidemic, just over 8000 patients spread out over 30 countries were infected with an overall mortality rate of 9.5% [69-70].

MERS has the potential to devastate parts of the world much like SARS did in 2003. Originally discovered in one man in Saudi Arabia [65], MERS cases have now been reported in 26 countries [69]. Most of these cases originated from people who had recently traveled to the Middle East [66]. Although no major epidemics have occurred to date [69], the recent outbreak in South Korea demonstrates the potential dangers of this virus. In July 2015, an outbreak affected 186 people, mostly via three major hospitals [71]. During that outbreak, more than 2,700 schools were forced to close, and over 16,000 people were put under quarantine [71]. The potential consequences of such an outbreak expanding into an epidemic are serious.

Although much is now known about the disease, there are still significant knowledge gaps. As mentioned previously, the mode of transmission is not well understood [67]. Another major knowledge gap is in the development of treatments to combat MERS-CoV. Currently, no approved antivirals or vaccines exist for MERS [67]. Over the years, a variety of candidates have arisen. Most notable is the monoclonal antibody m336, which demonstrates a potent ability to neutralize psuedoviral infection in cultured cells [72]. Unfortunately, until researchers are able to test these drug/vaccine candidates in a reliable animal model, development efforts will be severely hindered. This is why efforts to find or develop MERS models closely mimicking the human disease have increased dramatically over the past three years.

Because of the potential threat MERS poses, much work has been put into understanding how the virus infects host cells. Dipeptidyl pepdidase 4 (*DPP4*) was discovered as the receptor for MERS-CoV viral entry [73]. Since this initial discovery, crystal structures of the MERS-CoV receptor-binding domain (RBD) from the MERS spike protein, and the RBD in complex with

DPP4 have been solved [74-76]. The RBD consists of two subdomains. One subdomain is a

structural core that is structurally similar to SARS-CoV. The other subdomain is used for receptor

binding, and deviates significantly from the receptor binding subdomain structure of SARS-CoV

[74-76]. There is a species tropism for MERS-CoV, and *DPP4* plays a critical role in it [77].

Because of this, MERS-CoV is unable to infect common wild type rodents such as mice,

hamsters, and ferrets [77].

Current Animal Models for MERS

Since MERS was only just discovered in 2012 [65], few MERS animal models are

currently available. The first models developed and used were nonhuman primates (NHP).

Rhesus macaques infected with MERS virus developed lower respiratory infections along with

other clinical signs such as viral shedding, and slightly increased body temperatures [78-79].

These infections were generally mild and transient, with clinical signs beginning to resolve no

later than 3 days post infection [78-79]. Lung pathology was mild to moderate. Thus, these

Rhesus models are useful for studies of infection and mild to moderate disease, but are less useful

in studies of the severe form of the disease seen in humans [78].

Marmosets were also tested as a nonhuman primate MERS model. These animals

developed severe and persistent disease, with some animals needing to be euthanized due to

disease severity. The lung pathology was moderate to severe, and virus was detected in lung,

kidney, heart, and other tissues [80]. Conversely in another study that used two different isolates

of MERS-CoV, marmosets showed only mild to moderate signs of respiratory disease

accompanied by mild to moderate lung pathology. This study also saw no evidence of viral

dissemination unlike the first study [81]. Thus, the marmoset has been an inconsistent model for

MERS infection. For these reasons, the ethical concerns in using NHPs, and the high cost that

comes with NHP studies, there are extreme limitations in utilizing non-human primates to model MERS.

To address these limitations, work has been put into developing mouse models, which are less expensive to house and maintain. Unfortunately, as mentioned above, MERS is unable to bind to mice and other rodents' *DPP4* receptor [77]. In order to use mice or other rodents as a MERS model, a human *DPP4* needs to be expressed and present in lung tissue. The first h*DPP4*-MERS mouse model was made by transduction of adenovirus (Ad5) vectors expressing the h*DPP4* gene into mouse lung tissue. These mice developed interstitial pneumonia post infection [82]. The severity of the clinical presentation was dependent on the strain of mouse used, but ranged from mild to moderate. With this method, MERS mouse models could be generated in 2-3 weeks [82]. The labor and expenses involved in generating and housing these mice is much less than that of the non-human primate models. The main disadvantage to this model is that the infection is very short-lived. Even in immunocompromised mice, the MERS virus was cleared in 8-10 or 10-14 days, depending on the age of the animal [82]. Viral infection was also not fatal in these mice. This transient infection does not properly reflect the potentially deadly disease progression found in many human cases.

To generate a more severe model of the disease, two transgenic mouse models of MERS were developed. The first model contains an h*DPP4* transgene under the control of a CAG promoter resulting in global expression [83]. Transgenic mice developed moderate to severe clinical signs of pneumonia accompanied by progressive weight loss. Most mice died within 1 week post-infection [84]. Unlike the transduced model, this transgenic mouse model had a rapid, severe, and fatal disease progression. This progression is very useful in modeling severe human cases, but its usefulness in modeling moderate cases is limited. In addition to the lung, virus was also detected in the brain of these animals [84]. Although considered a respiratory disease,

neurological conditions have been observed in some severe human cases of MERS. It is still unclear if neural infection is a common aspect of the human disease [67, 85].

The second transgenic MERS mouse model contains a keratin 18 (K18) promoter controlling the h*DPP4* transgene [86]. This promoter preferentially expresses genes in epithelial cells, the primary cell types MERS-CoV infects in the lung [86]. K18-h*DPP4* positive mice presented with a lethal disease, dying 6-7 days post infection. Before death, these mice showed weight loss and a decrease in body temperature [86]. Both titers and viral RNA were detected at high levels in the brain and lungs [86]. There was a correlation between brain tissue infection and mortality in these studies [86]. Viral RNA but not virus titers was detected in the kidneys. Just like in the CAG-controlled transgenic mice, the K-18 controlled mice demonstrated lung and brain pathology after MERS infection [84, 86].

Currently there is one other MERS mouse model. Instead of transgenic, these mice were made susceptible to MERS by humanizing the mouse *DPP4* gene [87]. Lung pathology but not lethality was observed in this model after MERS infection. The presence of virus was limited to the lung, with no virus or pathology detected in the brain [87]. Overall this humanized mouse model seems to be a model of mild to moderate disease localized in lung tissue similar to the viral transduced model [82]. One thing to note about these animals is that these studies were only taken to 4 days post-infection. Other MERS model studies were taken to at least day 7 [87]. Because the humanized mouse studies were ended so quickly, it is unclear if these animals would develop a more severe disease with viral dissemination like in the transgenic mice [84, 86]. While these mouse models provide the opportunity to study the pathogenesis of MERS-CoV, knowledge learned from using this species cannot always be translated into humans [88]. Therefore, a hamster model for this emerging infectious disease will help to validate some of the findings made in mice and may provide some novel insights into the disease process. Furthermore,

creating an hDPP4/STAT2$^{-/-}$ hamster model will allow scientists to address the roles of STAT2-mediated innate immunity on virus control and disease progression.

Goats as Animal Models

The goat (*Capra hircus*) has proven to be a useful large animal model. Production of goat models is very reliable because techniques in husbandry and veterinary medicine are well established [89-91]. Additionally, the reproductive biology of goats is well understood [91]. Finally, the physiology and organ size between goat and humans are very similar [92]. Utilizing these advantages has resulted in the production of some useful disease models.

As summarized previously, goats have been used extensively in studying human heart diseases, especially AF [45]. Goats are also frequently used as models for human orthopedic conditions. Because of the similarity between the goat stifle and the human knee, they are considered one of the best models of ACL repair. They are also used to study other joint conditions such osteoarthritis [93]. The similarity between the goat stifle and the human knee have also allowed for the study of meniscal repair. Recently, the goat meniscus was used as a proof of concept for the use of guided tissue regeneration [94]. Goat scoliosis models have also been created [95].

Along with scoliosis, goats have been used to study other back conditions. The cauda equina is a bundle of nerves located in the lumbar vertebrae. Developing surgical techniques to repair injured cauda equina in smaller animals such as rats is difficult. Goats have a similarly sized cauda equina to humans that allowed for the development of a goat cauda equina repair model. In this model researchers were able to monitor the post-operative repair process more closely than in previous models [96].

Although orthopedics and surgical technique development has been the main use for goat models, they have also been used to study acute lung injury. The goat lung shares some similarity to the human one. For example, goat macrophages produce very little nitrous oxide just like human macrophages do [97]. Additionally, measuring protein concentration in blood lymph, a key parameter in assessing acute lung injury, is well established in goats [98]. Some bacterial infections have also been studied in goat models. Goat models have been developed for both listerosis and *Clostridium perfingens* infection. In both of these models, disease progression and pathology was extensively studied [99-100].

Hamsters as Animal Models

The original stock of golden Syrian hamsters (*Mesocritus* auratus) was acquired from Jerusalem in the 1930s. Since their initial capture a variety of colonies have been developed [101-102]. These colonies have been used to study a wide variety of diseases such as dental caries, diabetes, hypertension, and muscular dystrophy [102]. Hamsters can be generated relatively quickly because of their 15-18 day gestation period [103-104]. They are also easy to handle, usually showing aggression only when startled or woken suddenly [104].

One of the most advantageous aspects of using the hamster model is how closely their disease progressions are to those of humans for many conditions. For example, in the hamster cheek pouch oral cancer model, many of the disease stages match the human progression [105-106]. The cardiomyopathic model (CM) hamsters are another set of well-established specialized hamster models. These lines of hamsters all exhibit a similar disease progression, and have been used to study a variety of cardiac conditions such as cardiomyopathy and atherosclerosis [107-108]. Recently the BIOF1B hamster, one of these CM colonies, has been of particular interest. These animals have been used to study artherosclerosis, the effects of fish oil on lipid metabolism,

and the contribution of inhibitory G-proteins in the development of heart disease [12, 109-110]. This line of hamsters is especially advantageous because, unlike mouse atherosclerosis models, hamster lipid metabolism is very similar to humans, involving many of the same enzymes. These include the LDL receptor, apolipoprotein E, and CETP [12].

Wild type golden Syrian hamsters are also being extensively used in modeling human viral infections. They have been previously used to study the deadly SARS coronavirus [111], and are showing promising signs for use in Ebola and other hemorrhagic fevers [112]. Hamsters infected by mouse adapted Ebola virus show hallmark symptoms and pathology as compared to humans [113].

In addition to hemorrhagic fevers, hamsters have also shown promise in being better models of adenovirus infections. Hamsters have been shown to be susceptible to adenovirus infection, and also allow viral replication [114]. Oncolytic adenoviruses have recently shown promise in becoming a cancer treatment. Because of their susceptibility to adenoviral infection, and their ability to allow robust replication, hamsters have also become a frontrunner for testing oncolytic viral treatments for various types of cancer [114].

Despite their many advantages, there have been major limitations preventing the more extensive use of hamsters as animal models. The first is the lack of hamster specific immunological assays, which may limit researchers in their abilities to study disease progression, immune response, and pathology [114]. Currently work is being done to overcome this setback. qRT-PCR assays for various hamster host response genes have been developed and validated [115]. The Wang laboratory is currently leading an effort to form an international golden Syrian hamster consortium to develop and share hamster-specific reagents for use in hamster modeling studies.

Another roadblock that is currently being overcome is the lack of a complete hamster genomic sequence. A complete transcriptome is now available [116], but there is no complete

hamster genomic sequence. This limitation is being addressed by choosing the Syrian hamster as one of the 27 high priority Eutherian mammals for whole-genome sequencing by the Genome 10K project. The first draft assembly was recently completed [117].

The most significant roadblock in using hamster models more extensively was the lack of gene-targeting tools in this species, which has been recently overcome by the Wang laboratory [118]. Up until recently, there was no gene-targeting system to use in hamsters. From a genetic standpoint, this limited the use of hamster models to diseases that can be mimicked in the wild type hamsters. In 2014, Fan, *et al* was able to generate genome-edited hamsters using the CRISPR/Cas9 system. They were able to target a few different genes, but the highlight from this work was the generation of the *STAT2* knockout hamster [118].

STAT2 is a signaling protein in the type I interferon (IFN) pathway, a key component in the innate immune response. The previously mentioned *STAT2* KO hamster contained a 1-nucleotide insertion in the N-terminal domain of the *STAT2* gene, which fully abolishes the expression of *STAT2* protein. When these hamsters were infected with human adenovirus 5 (Ad5), they showed higher viral loads in the liver, lungs, and kidneys compared to wild type controls. The *STAT2* KO hamsters also had a much higher mortality rate as a result of infection [119]. This was the first study in which researchers could investigate the immune responses relevant to late-phase Ad infection in animal models, as previous mouse models were unable support adenoviral replication [119]. The *STAT2* KO hamsters also demonstrated the importance of type I IFNs in the immune response against adenoviral infection [119].

The *STAT2* KO hamster is the first example of a genetically modified Syrian golden hamster [118]. This is a major breakthrough in studying adenovirus pathology, but more importantly, in the use of hamster disease models. With this newly developed hamster gene-modifying platform, hamster animal models can be generated to precise specifications.

CRISPR/Cas9: A New Tool to Efficiently
Develop Precise Animal Models

In the past, gene targeting has been inefficient and labor intensive. Traditional gene targeting requires the generation of a targeting vector containing a modification of choice, and homologous arms at least thousands of nucleotides long. This vector is inserted into cells and relies on homologous recombination to modify DNA. This process is labor intensive, and inefficient. Modification efficiency has been reported to be as low as <1%, and as high as 10% [120-121] This technique requires selection of edited cells, which often requires the insertion of foreign components such as a GFP gene or an antibiotic resistance gene to facilitate selection [122-124].

One of the greatest innovations in gene functional studies and animal model generation has been the development of precise gene-targeting technologies. Zinc finger nucleases, TALEN, and CRISPR/Cas9 have all made genome editing both rapid and customizable [125-126]. The principle components behind these technologies are protein-DNA or RNA-DNA interactions for precise targeting, and an endonuclease that makes a double stranded break at the DNA target [126]. After the double stranded break, the cell repairs itself via non-homologous end joining (NHEJ) or homologous recombination (HR). When NHEJ is used, frameshift mutations are induced. These mutations often result in the formation of a premature stop codon, thereby producing a gene KO. Introducing a donor oligonucleotide containing homologous arms will induce HR. The center of this donor sequence will contain mutations ranging from single point mutations to mutations many nucleotides long [126].

Originally found in bacteria as a viral defense mechanism, CRISPR/Cas9 (Clustered Regularly Interspaced Short Palindromic Repeats) has been utilized as a genome editor that has been widely used in many organisms including: mice, rats, goats, and human embryonic stem cells [127-130]. The guide RNA sequence (sgRNA or gRNA) acts as the DNA binder, interacting

with its target via complimentary base pairing. The endonuclease in this system is Cas9, which

is guided to the target site by forming a complex with the sgRNA [127-128]. The only constraint

on what sequences CRISPR can target is the PAM (Protospacer Adjacent Motif) sequence.

Recognition of this three-nucleotide long sequence is required for Cas9 binding and cleavage

[131-132]. In order for a gRNA sequence to bind to its target, the target must be followed by a

PAM sequence on the 3' end. The exact sequence of the PAM can vary, but in the most

commonly used CRISPR systems the PAM is any nucleotide followed by two Gs (NGG) [127].

CRISPR/Cas9 genome editing is rapid and efficient with reported efficiencies being as

high as 65-77% [133-135]. This system is also customizable, unlocking the potential for precise,

efficient, and quick generation of animal models. Currently, there are two commonly used ways

to generate animal models using CRISPR/Cas9. The first is via cloning by somatic cell nuclear

transfer (SCNT). In this procedure, a population of cells is first edited by CRIPSR/Cas9. Next,

cell lines from these populations are established via serial dilution. Once cell lines are screened

for a mutation of interest, positive colonies can be used as nuclear donors for SCNT. The

resulting cloned animals will contain the genomic modification induced by CRISPR/Cas9 [133].

Using this technique, CRISPR/Cas9 edited goats and pigs have been generated [129, 133].

CRISPR/Cas9 edited bovine cells have also been used for SCNT. These clones could be cultured

to the blastocyst stage allowing for the potential to produce genetically engineered cows using

this method [134].

The second strategy commonly used is direct editing of the zygote. In this strategy, the

CRISPR/Cas9 components are directly injected into a zygote by a procedure known as pronuclear

(PN) injection. The zygote is microinjected with either the sgRNA/Cas9 plasmid or mRNA of

both Cas9 and the sgRNA [135-137]. After injection, embryos are implanted into a female

recipient. Since the single-celled zygote is edited, all daughter cells contain the same modification.

This strategy was used to generate the *STAT2* KO hamsters discussed above [118]. This strategy

has been used in smaller organisms including mice previously [133-137], but has recently been adopted for use in larger animals including sheep, goats, and pigs [138-141]. Considering the fact that SCNT technology has not been successfully applied to some animal species, such as the Syrian hamster, conducting gene editing in zygotes made it possible to create genetically engineered animals in these species.

With the development of genome engineering technologies such as CRIPSR/Cas9, it has never been easier to efficiently produce genetically engineered animals for use in gene studies and animal model development. Atrial fibrillation, long qt syndrome, and MERS are all deadly diseases with a need for the development of alternative genetically engineered animal models. In this thesis project I have laid the foundations for producing LQT1 goat models, LQT1 and AF hamster models, and MERS-CoV hamster models.

CHAPTER II

OBJECTIVES

- Generate *KCNQ1* knockout mutations using CRISPR/Cas9 for the purpose of generating LQTS animal models:

  o In goat fibroblast cells

  o In hamsters

- Use CRISPR/Cas9 to induce the *KCNQ1* gain-of-function knockin mutation, Q147R, in hamster cells to produce a hamster model of AF.

- Establish h*DPP4* positive hamsters in the *STAT2* KO background via crossing h*DPP4*$^{+}$ hamsters with *STAT2* knockout hamsters to produce a hamster model of MERS-CoV.

CHAPTER III

METHODS

AF and LQTS Model Development

Cell Culture

For *in vitro KCNQ1* knockout and gain-of-function knockin, goat fetal fibroblast (GFF) cells (provided by Dr. Irina Polejeva) established from gestation day 40 to day 60 fetuses and baby hamster kidney cells (BHK-21 (C-13; ATCC) were used. These cells were grown and maintained in Dulbecco Modified Eagle Medium supplemented with 10% fetal bovine serum (v:v), 1% penicillin/streptomycin, and 1% non-essential amino acids (Life Technologies). Cell incubation temperatures were 37.5 and 37 degrees Celsius for the goat cells and hamster cells, respectively. Both incubation environments contained 5% CO_2 in the air.

Animal Work/Ethics Statement

Golden Syrian hamster production, maintenance, and PN embryo manipulations are described in Fan *et al* [118]. Briefly, founder animals were purchased from Charles River Laboratories. Hamsters used for PN embryo production were bred in-house. Wild type females used as embryo transfer recipients were generated from a breeding colony established in the Wang laboratory. Hamsters were raised in an air-conditioned room with a 14-hour light and 10-hour dark light cycle (14L:10D; 6:00 am light on, 8:00 pm light off). The experiments performed were in accordance with guidelines of the AAALAC-accredited Laboratory Animal Research Center at Utah State University and approved by the Institutional Animal Care and Use Committee of Utah State University (IACUC Protocol: 2484).

***KCNQ1* Characterization**

Genomic DNA isolation was performed on cultured cells using the Puregene Core Kit A according to the manufacturer's instructions (Qiagen). Published *KCNQ1* genomic sequences of hamster (NW_004801604.1) and goat (NC_022321.1) were used to design PCR primers that amplify regions of hamster *KCNQ1* exon 2 (HaKCNQ1F1: 5'tgagtgcactagctgaggga3'; HaKCNQ1R1: 5'aatctgggctgggacacttg3') and goat *KCNQ1* exons 1 (KCNQ1Ex3F: 5'ttgtcctggcctgcctcatc3'; KCNQ1KIR1: 5'ccgtcattcttccgccttctca3') and 2 (Kcnq03: 5'gagatcgtcctggtggtgttcttcg3'; gsR1: 5'cagtggacactcctattgtgctgag3'). 50-200 ng of genomic DNA isolated from goat fetal fibroblasts was amplified by polymerase chain reaction (PCR) using ExTaq (Takara) with 10 pmol of forward primer and 10 pmol reverse primer in each PCR reaction. Thermocycler protocol started with a 3 min. melting step (94° C), followed by 38 cycles of melting (94° C for 30 s), annealing (60° C for 30 s), and extension steps (72° C for 30 s). A final extension step was used (10 min. at 72° C). 10 pmol of each primer pair was used in each reaction.

BHK genomic DNA was PCR amplified in a similar fashion as in the goat. ExTaq was used to amplify 50-200 ng of template using 10 pmol of each *KCNQ1* exon 2-specific primer. Thermocycler protocol was exactly the same as the above goat protocol except that the annealing temperature was 64° C, and the extension time was for 1 min instead of 30 s. Depending on the specificity of the PCR reaction, the resulting PCR products were purified by either gel extraction or PCR purification according to manufacturer's instructions (Qiaquick kits, Qiagen). Purified PCR products from both goats and hamsters were then sequenced via Sanger sequencing. These sequences were used to design sgRNA targets for the above loci. These targets were found according to the $G(N)_{20}GG$ motif.

Gene Targeting in GFF and BHK Cells

To target the *KCNQ1* genomic loci mentioned above in GFF and BHK cells, pX330-U6-Chimeric_BB-CBh-hSpCas9 plasmids (Addgene ID: 42230) were constructed as described previously [127]. DNA oligo templates for the sgRNA targeting sites were synthesized by Integrated DNA Technologies (IDT, Iowa, USA). Between 7.5 X 10^5 and 10^6 cells were transfected with 5 μg (GFF cells) or 2-4 μg (BHK cells) of sgRNA/Cas9 vector plasmid DNA. Transfections were performed using AMAXA 4D nucleofection (Program EN-150). For gain-of-function knockin experiments on BHK cells, 26 μg of PAGE purified single stranded DNA donor oligo (IDT) containing the one nucleotide mutation of interest, a one nucleotide mutation to disrupt the PAM sequence, and 142 nucleotides of homologous arms was cotransfected with the sgRNA/Cas9 vector into the cells. 48-72 hours post-transfection, cells were harvested and isolated for genomic DNA using the Puregene Core Kit A according to the manufacturer's protocol (Qiagen). Isolated genomic DNA was amplified for the above genomic loci using the same PCR protocols described earlier.

If the resulting PCR products were a single intense band of the correct size, then they were digested directly by restriction enzyme without prior purification. The digested products were resolved on 2% agarose gel stained with SYBR Safe DNA stain (Life Technologies). Since CRISPR/Cas9 targeting abolishes the chosen enzyme sites, the PCR product's ability to resist digestion determined weather gene knockout events occurred. Conversely, the gain-of-function mutation in BHK cells creates a new enzyme site (BsrBI) leading to the presence of digest products. Targeting efficiency was estimated by measuring the relative intensity of the digest-resistant band to the digested bands. This measurement was determined using Image J software (1.47p, NIH).

SURVEYOR Nuclease Assay

SURVEYOR Nuclease assay was also used to detect knockout events in BHK cells. *KCNQ1* targeted and wild type PCR fragments were mixed together and run on a hybridization reaction according to manufacturer's protocol. The resulting heterogeneous dihybrids were digested with SURVEYOR nuclease at 42° C for 1 hour. After stop solution was added to the hybrids, digested products were resolved on a 1.5% agarose gel stained with SYBR Safe. Hybrids that included a strand that had been edited would produce mismatches in the hybrids that SURVEYOR nuclease exclusively cuts.

**PCR Based Detection of *KCNQ1* Gain-of-Function
Mutations in BHK Cells**

In addition to enzyme digest, *KCNQ1* gain-of-function knockin mutations were also detected using PCR. A new forward primer containing the *KCNQ1* gain-of-function substitution at the 3' clamp allowed it to amplify BHK genomic DNA with the substitution mutation, but not wild type DNA (Ha*KCNQ1* KI Q147R: 5'ctgtccactattgagcg3'). Using this primer and primer HaKCNQ1R1, wild type BHK genomic DNA was subjected to PCR amplification according to the protocol described above using a gradient of annealing temperatures (Ta's shown in Figure 16) to establish its selectivity against wild type DNA. I established a PCR-based assay that a 380 nucleotide PCR product was generated from genomic DNA with the gain-of-function knockin mutation, but no PCR product resulted from wild type genomic DNA at an annealing temperature of 58° C.

Cell-Line Establishment

48 hours post-transfection, GFF and BHK single cell derived colonies were established via limiting dilution. The diluted cells, at the concentration of 10-15 cells per ml, were plated into 96-well plates with each well receiving 200 µl of cell suspension. Cell culture plates were

checked under inverted microscope every 2-3 days to identify and mark the wells containing

single cell colonies. After 10-14 days (media changed every 4 days), single cell derived colonies

that reach confluency were transferred to 24-well plates, and grown to 80-90% confluency. At

this point, half of the cells were harvested for genomic DNA isolation and screened for mutations

by PCR followed by enzyme digest using the techniques described above, or by directly

sequencing the PCR products. The other half were passaged into either fresh 24-well plates or 12

well plates. After the passaged cells were grown to 80-90% confluency, cells that were positive

for knockout mutations were cryogenically frozen in liquid nitrogen. To determine the exact types

of mutations produced in both GFF and BHK cells, PCR products of cell lines that were knockout

positive were cloned into TA vectors (Invitrogen). TA clones were sequenced via Sanger

sequencing.

MERS MODEL DEVELOPMENT

Vector Construction

The GFP reporter gene used here originated from the pEGFP-N1 plasmid (Addgene ID:

6085-1). HindIII-E2A-GFPF

(5'gg<u>aagctt</u>ccaatgtactaactacgctttgttgaaactcgctggcgatgttgaaagtaatcccggtcctatggtgagcaagggcgaggag

ctgttc3'; underlined sequence is the HindIII recognition site) and GFPR-XbaI

(5'gg<u>tctaga</u>ttacttgtacagctcgtccatgc3'; underlined sequence is the XbaI recognition site) primers

were used to create and amplify the E2A-GFP cassette. E2A-GFP cassette was cut by HindIII and

XbaI and was sub-cloned into the pDNR-DPP4 plasmid (DNASU ID HsCD00021611) at the

HindIII/XbaI sites. The resulting DPP4-GFP cassette was amplified with a forward primer

containing an XbaI site and a reverse primer containing a NotI site. The amplified XbaI-DPP4-

GFP-NotI cassette was inserted into the pK18-tTs plasmid (provided by Dr. Stanley Perlman). tTs was replaced by the DPP4-GFP cassette via XbaI/NotI ligation to create pK18-DPP4-GFP.

The K18-DPP4-GFP cassette was then liberated from the above resultant plasmid by SpeI and BamHI. PiggyBac Vector (PB513B-1, Systems Biosciences) was opened by the same restriction enzymes. The K18-DPP4-GFP cassette was inserted into the PiggyBac vector using SpeI/BamHI ligation, creating the PB-DPP4-GFP intermediate vector. The intermediate vector was then cut by NruI and BamHI to eliminate the PiggyBac elongation factor (EF1) and GFP. This allows for GFP expression to be under the control of the K18 promoter instead of being constitutively expressed. The final PB-DPP4-GFP vector free from EF1 and GFP was self-ligated together via blunt-end ligation.

hDPP4 X STAT2 Crosses

Transgenic hDPP4 hamsters were generated by pronuclear injection of PB-DPP4-GFP and PiggyBac Transposase (PB210PA-1) vectors in-house (unpublished). STAT2 KO hamsters were generated previously by Fan *et al* [118]. Housing conditions for the hamsters are described above.

Hamsters with hDPP4 genotype (DPP4$^{+/-}$) were crossed with hamsters containing a loss of function STAT2 allele (STAT2$^{+/-}$). To cross these animals, females on day four of their estrous cycle were placed in the male cage, and the two animals were observed to make sure they did not fight each other. Once mating began, the mating pairs were left alone for one hour, and then separated back into their own cages. Two to three weeks after pups were born, toe clippings were taken and used to isolate genomic DNA using the Pure Gene Core Kit according to the manufacturer's protocol (Qiagen). Sister/brother breeding was then performed in order to produce hDPP4 positive hamsters that were homozygous for the STAT2 knockout allele (DPP4$^{+/-}$; STAT2$^{-/-}$).

hDPP4 Genotyping

DPP4 genotyping was performed using genomic DNA PCR. 100-500 ng genomic DNA was amplified using ExTaq (Takara). Thermocycler protocol started with a 3 min. melting step (94° C), followed by 35 cycles of melting (94° C for 30 s), annealing (64° C for 30 s), and extension steps (72° C for 1 min). 10 pmol of each primer (K18 F2-1: 5'gccacttaccttgcaagcac3'; K18 R2-1: 5'cgccagcgagtttcaacaaa3') was used in each reaction. PCR products were visualized on 1.5% agarose gels stained with SYBR Safe. Samples containing the hDPP4 gene produced a 658 nucleotide PCR product.

STAT2 Genotyping

STAT2 genotyping was performed by first producing an 869 nucleotide PCR product using Phusion high-fidelity polymerase (Thermo-Fisher). Thermocycler protocol started with a 3 min. melting step (98° C), followed by 35 cycles of melting (98° C for 10 s), annealing (65° C for 30 s), and extension steps (72° C for 30 s). 10 pmol of each STAT2-specific primer (E03: 5'gtacagggaagagctggaactgatg3'; E04: 5'ctgtatcctctgtgacacttgccac3') were used to amplify 100-300 ng of genomic DNA template per reaction. 5 μl of the resulting PCR products were directly digested with fast digest BglII (Thermo-Fisher). Digested products were resolved on a 1.5% agarose gel stained with SYBR Safe. The STAT2 knockout mutation abolishes the BglII site, rendering the PCR products resistant to digest by which the STAT2 knockout allele and wild type allele can be distinguished. PCR products completely resistant to digest were determined to be homozygous for the knockout genotype (STAT2$^{-/-}$), while PCR products that are semi-resistant (half of a product can be digested by the BglII restriction enzyme) indicate the heterozygous knockout genotype (STAT2$^{+/-}$

CHAPTER IV

GENETIC KNOCKOUT OF GOAT *KCNQ1* WITH THE CRSPR/CAS9 SYSTEM

Goat *KCNQ1* Characterization

We decided to knock out the goat *KCNQ1* by introducing frameshift mutations in exon 1 of this gene via the CRISPR/Cas9 system. Additionally, we chose to target exon 2 as an alternative knockout strategy. Targeting the first exons of the gene will fully abolish the function of the goat *KCNQ1* gene. Another reason to target exon 1 is that it corresponds to the human *KCNQ1* exon 2 (see below) where three gain-of-function mutations have been identified in families with a history AF or in patients presenting with AF [35-36, 38]. Designing a gene knockout vector in this locus will allow for future experiments to generate knockin edits in this same region using the same gene-targeting vector.

Designing gene-targeting vectors to genetically knock out the goat *KCNQ1* requires characterization of the genomic sequence of the goat gene. DNA sequence alignment analysis based on the published goat and human *KCNQ1* sequences showed that Exon 2 of the human *KCNQ1* mRNA sequence (NM_000218.2) aligns to exon 1 of the goat *KCNQ1* gene (NC_022321.1) in the goat genome assembly (Fig. 1 A). Goat *KCNQ1* exon 1 and some of the downstream intron sequence was PCR amplified from genomic DNA isolated from one of the goat fetal fibroblast cell lines we are working with and sequenced. The resulting sequence was an exact match to the published sequence within the exon, but differed significantly in the intron sequence (Fig. 1A). Similar results were obtained when the *KCNQ1* exon 2 locus was amplified and sequenced (Fig. 1B). From these sequencing data, contigs of two goat *KCNQ1* loci were generated, and were the basis for guide RNA (gRNA) template designs.
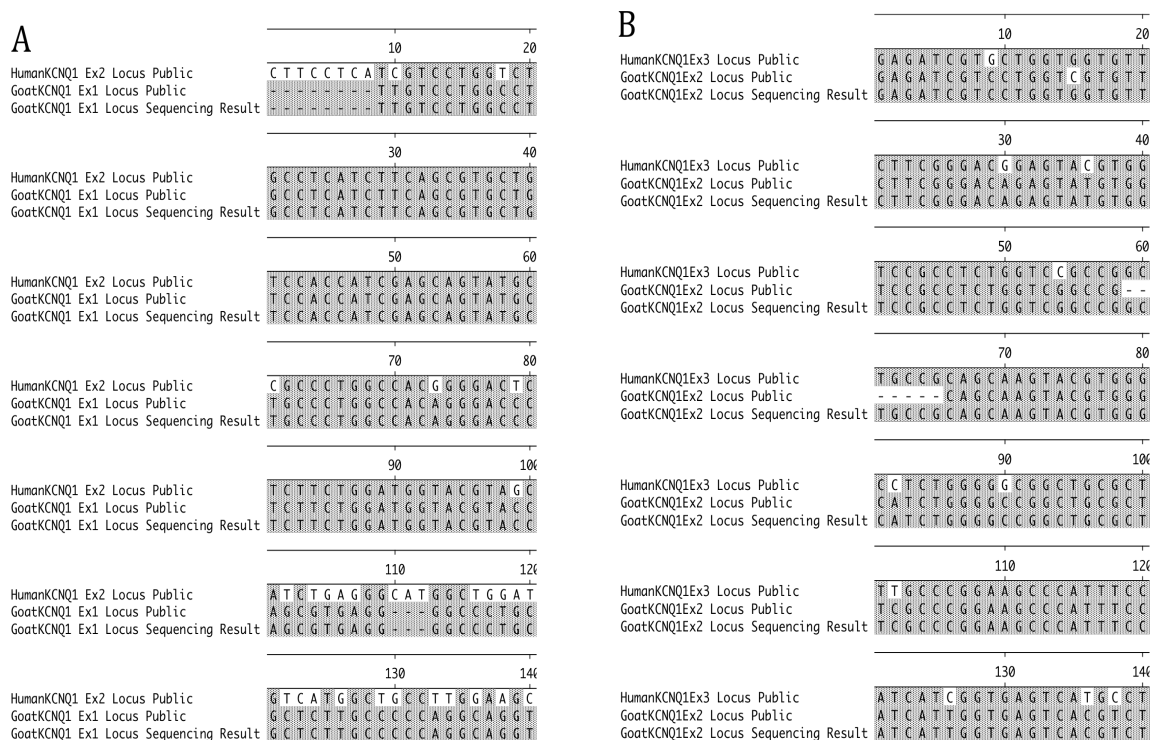
Fig. 1 Sequence characterization of goat *KCNQ1* targeting loci. Sequenced *KCNQ1* loci of goat exons 1 and 2 were aligned to the corresponding publicly available human and goat sequences (NM_000218.2 & NC_022321.1 respectively). Shaded areas represent 100% sequence identity to the consensus sequence. A) The goat exon 1 locus corresponds to human exon 2 (1-91) with a sequence homology of 73% for the whole locus. B) The goat exon 2 locus corresponds to human exon 3 (1-127). Sequence homology for the whole locus equals 90%

Fig. 2 Schematic of goat *KCNQ1* targeting locations. Locations of CRISPR/Cas9 cut sites (stars) and PCR primers (arrows) are displayed in the genomic context of goat *KCNQ1*.

KCNQ1 Gene-targeting in Goat Fibroblast Cells

Two *KCNQ1*-targeting gRNAs were designed: one that targets exon 1 (*KCNQ1*Ex1) and one that targets exon 2 (*KCNQ1*Ex2) (Fig. 2). To knock out the *KCNQ1* gene in a goat fibroblast

cell line, plasmids expressing Cas9 and one of the gRNAs (sgRNA/Cas9 vector) were

transfected into the goat fetal fibroblast cells. Forty-eight hours post-transfection, genomic DNA

from the transfected cells was isolated to examine gene-targeting events and efficiency using

RFLP assays (Table 1, Fig. 3). For *KCNQ1*Ex1, bulk cell RFLP yielded an estimated efficiency

of 30 % (data not shown). CRISPR gRNA targeting exon 2 had a better targeting efficiency,

which was estimated to be as high as 53% (Fig. 4).
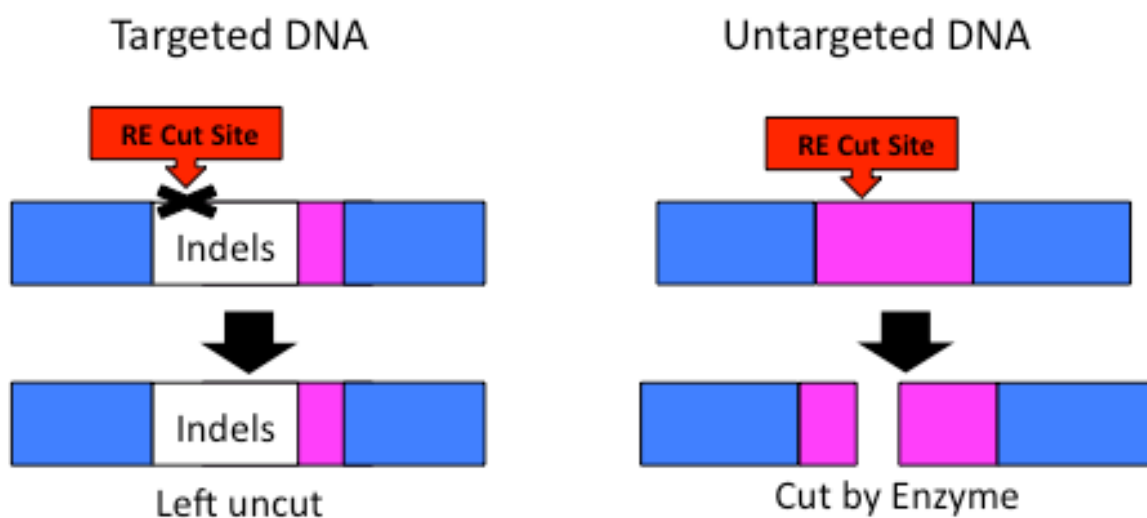
Fig. 3 General schematic of RFLP analysis. Targeted DNA is repaired by NHEJ, abolishing a
restriction enzyme recognition (RE) site in the process. Untargeted DNA will be cut by the
restriction enzyme. This can be viewed as digested and undigested DNA on a gel.

Table 1 CRISPR/Cas9 gRNA's used for goat *KCNQ1* knockout

gRNA Name	gRNA Sequence (5'-3')	Exon Targeted	F Primer (5'-3')	R Primer (5'-3')	RE Used
KCNQ1 Ex1	GTGGCCACAGGG ACCCTCTTCTGG	1	TTGTCCTGG CCTGCCTCA TC	CCGTCATTCT TCCGCCTTCT CA	EarI
KCNQ1 Ex2	GGCTGCCGCAGC AAGTACGTGGG	2	GAGATCGTC CTGGTGGTG TTCTTCG	CAGTGGACA CTCCTATTGT GCTGAG	BsaAI

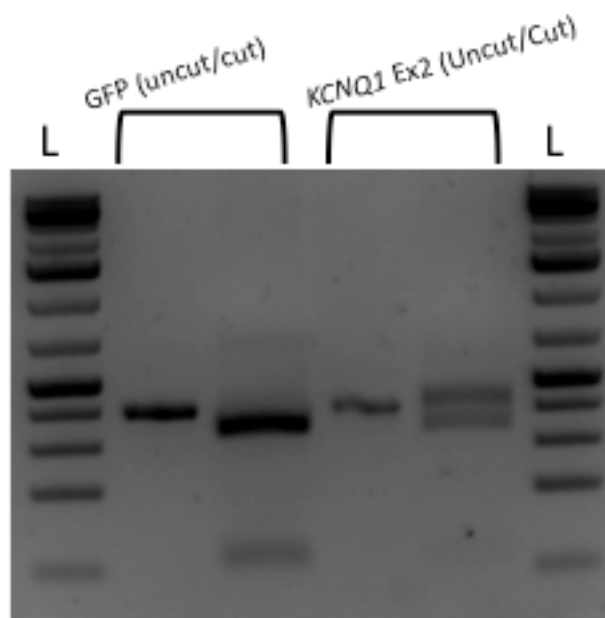**Fig. 4 RFLP analysis of *KCNQ1Ex2* knockout efficiency.** DNA from *KCNQ1Ex2* transfections produced a band resistant to BsaAI digestion unlike the GFP transfected control DNA. Targeting efficiency was estimated to be 53%.

Establishment of Single Cell Derived Colonies

Based on the results obtained from bulk cell analysis, cells targeted by the exon 2 gRNA were chosen to establish single cell-derived colonies by limiting dilutions. Of the 15 colonies screened, three (3-E3, 5-D3, and 5-G4) were shown to have indels at the targeted site. PCR product sequencing of colony 5-E3 showed a 28-nucleotide deletion on both alleles (Fig. 5).

The other two colonies, 5-D3 and 5-G4, were shown to have multiple indel types due to double peaks in the chromatograms at the targeting site (Fig. 6A). Indel types were determined by sequencing TA clones made from PCR products. These two colonies had alleles with 28-nucleotide deletions and 11-nucleotide deletions (Fig. 6B). Surprisingly, all three colonies contained the exact same 28-nucleotide deletion, and colonies 5-D3 and 5-G4 had identical 11-nucleotide deletions. This was unexpected, as indels produced by NHEJ occur independently

from cell to cell. These data suggest a possible cell type- or locus-specific NHEJ event that occurred in these three colonies. More experiments would need to be performed to determine the exact mechanism of these identical indel events.
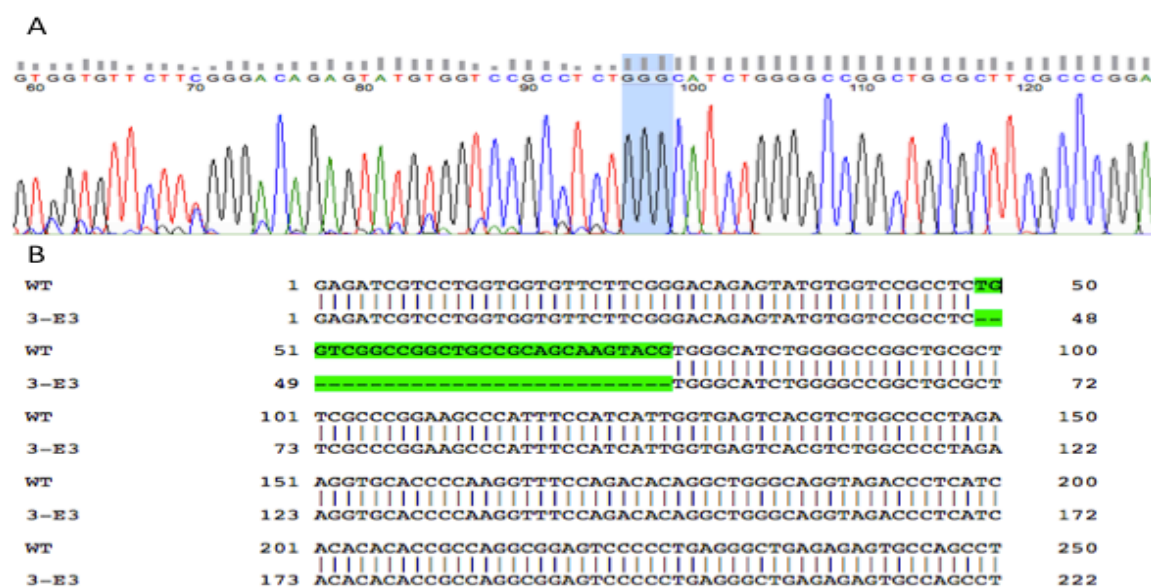

Fig. 5 Colony 3-E3 contains a 28-nucleotide deletion. A) Partial chromatogram generated from gDNA PCR of colony 3-E3 followed by Sanger sequencing as described in methods (PAM highlighted blue). B) Alignment to the wild type (WT) sequence shows a 28-nucleotide deletion at the CRISPR/Cas9 target site (highlighted in green).

Conclusions and Ongoing Efforts

I successfully characterized regions of goat *KCNQ1* exons 1 and 2 via genomic PCR and sequencing. For both *KCNQ1Ex1* and *KCNQ1Ex2* loci, my sequences had a 100 and 95% sequence homology to the published goat sequences respectively. Sequence homology to the published human *KCNQ1* loci were 73% (goat exon 1) and 88% (goat exon 2) Since the exons are conserved between goats and humans at these loci, my acquired sequences were used to design sgRNA/Cas9 expression vectors targeting these regions of goat *KCNQ1*. Both gRNAs that

were designed were able to cleave their designated target and induce indels. *KCNQ1*Exon2 had

a higher indel efficiency, and therefore was chosen to be used for cell line establishment.
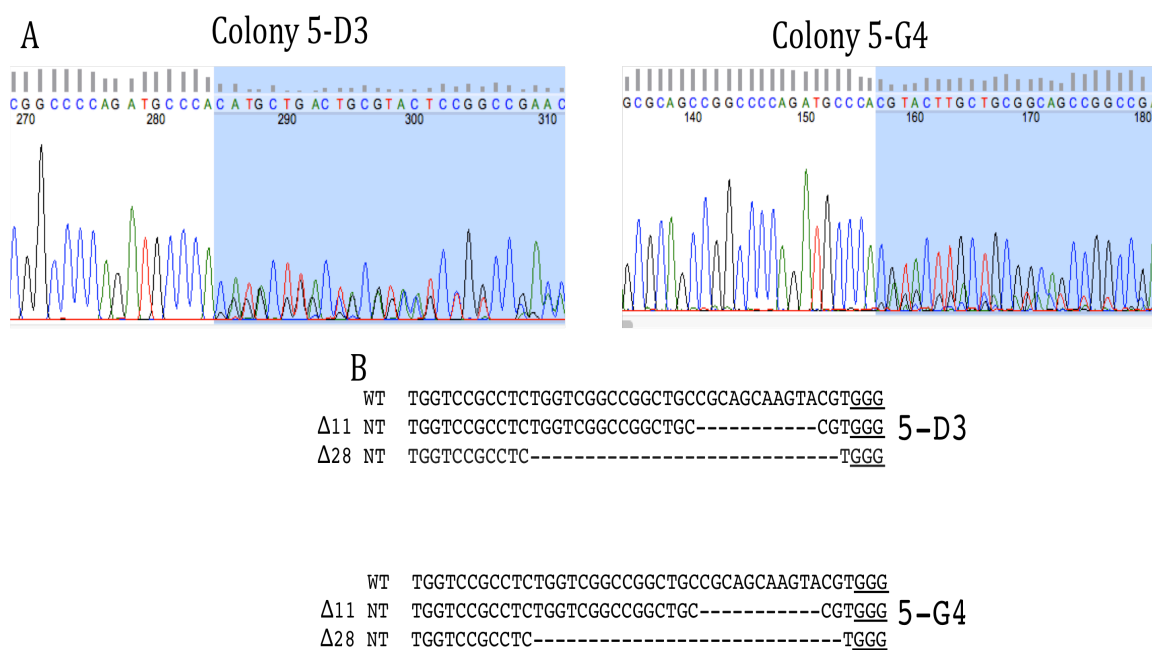
Fig. 6 Colonies 5-D3 and 5-G4 have identical indels. A) Sequencing chromatograms of PCR products contain double peaks starting at the CRISPR/Cas9 *KCNQ1*Ex2 targeting site (blue highlight). B) Alignments of 5-D3 and 5-G4 clones yield identical 11 and 28-nucleotide deletions. Interestingly, the 28-nucleotide deletions here are identical to the deletion observed in colony 3-E3 (Fig. 5).

Collectively I screened a total of 15 colonies transfected with the *KCNQ1*Ex2

sgRNA/Cas9. Three of them had indel mutations yielding an efficiency of 20%. It is interesting to

note that all three cell lines shared the same 28-nucleotide deletion, and two of them shared an

identical 11-nucleotide deletion (Table 2). As we have also observed similar phenomena

targeting the hamster genome with the CRISPR/Cas9 system, it may be possible that the NHEJ

machinery makes consistent indels at this particular locus due to these types of repair being

preferred thermodynamically.

Table 2 Cell lines generated from *KCNQ1Ex2* transfection into goat fetal fibroblasts

I.D.	Transfected With:	Screening Results	Comments
3-E3	*KCNQ1Ex2*	PCR product sequencing showed a biallelic 28 nucleotide deletion	None
5-D3	*KCNQ1Ex2*	TA cloning/Sequencing of PCR product showed 11 and 28 nucleotide deletions	28 nucleotide deletion identical to 3-E3; 11 nucleotide deletion identical to 5-G4
5-G4	*KCNQ1Ex2*	TA cloning/Sequencing of PCR product showed 11 and 28 nucleotide deletions	28 nucleotide deletion identical to 3-E3; 11 nucleotide deletion identical to 5-D3
Totals	3/15 colonies screened contained knockout indels. Targeting efficiency= 20%		

The cell lines generated from these efforts contain indels that will cause frameshift mutations leading to premature stop codons, resulting in a non-functional *KCNQ1* protein (Fig. 7). These knockout cell lines can be used as nuclear donors for SCNT. We chose to use SCNT to clone genetically engineered goats, instead of using PN injection because we have a ongoing goat cloning program for other research projects at USU (Drs. Kenneth White and Irina Polejaeva's laboratories). Clones generated from these donors will contain the same *KCNQ1* KO mutations. These knockout goats should make excellent models of LQT1. Efforts to induce other types of *KCNQ1* knockout mutations are ongoing. Recently, I transfected more *KCNQ1* goat fibroblast cells with *KCNQ1*Ex1 and *KCNQ1*Ex2 CRISPR plasmids. Genotyping of these transfections and single-cell derived colony establishment is currently in progress.

Fig. 7 Goat _KCNQ1Ex2_ knockout mutations lead to premature stop codons. A) The 11-nucleotide deletion produces a premature stop codon (TGA) at position 577. B) The 28-nucleotide deletion produces a premature stop codon (TGA) at position 1015. Goat _KCNQ1_ mRNA CDS is 2405 nucleotides long (XM_013976076.1).

CHAPTER V

GENETIC TARGETING OF THE HAMSTER *KCNQ1* GENE

Hamster *KCNQ1* Characterization

We were interested in targeting the same region of human *KCNQ1* in hamsters as we did in goats. Human *KCNQ1* exon 2 (NM_000218.2) aligns with exon 2 of the hamster genome assembly (NW_004801604.1) (Fig. 8). Targeting this gene region allowed us to generate both knockout (for LQTS1) and gain-of-function mutation knockin (for AF) hamsters. For knockin generation, we were interested in the Q147R mutation; a well-characterized familial gain-of-function mutation that causes AF [38]. It was recently found that a patient carrying this mutation also presented with a prolonged QT interval [38]. In the human *KCNQ1* gene, an A to G substitution results in the Q147R gain-of-function mutation. Designing a CRISPR at this locus allows for both targeted gene knockout and knockin using the same CRISPR.
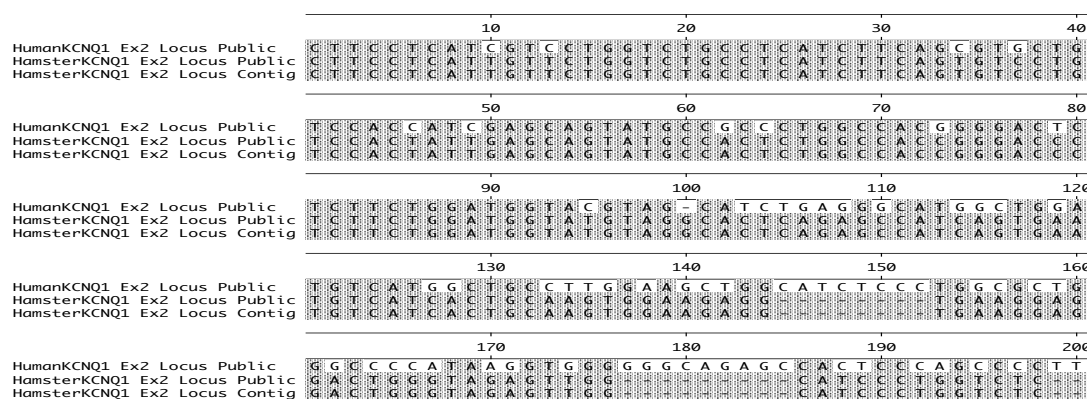
Fig. 8 Characterization of hamster *KCNQ1Ex2* locus. Sequenced *KCNQ1* locus of hamster exon 2 was aligned to the corresponding publicly available human and hamster sequences (NM_000218.2 & NW_0048801604 respectively). Shaded areas represent 100% sequence identity to the consensus sequence. Predicted and sequenced hamster loci share 100% homology with each other. Exon 2 (position 1-91) is well conserved (89% homology) between human and hamster, including the Q147R A to G substitution location (position 54).

The hamster *KCNQ1* locus was amplified from Baby Hamster Kidney (BHK) cell gDNA using primers flanking the 91-nucleotide long exon 2 plus some of the surrounding intron sequence (Fig. 9). Sanger sequencing showed that this PCR product aligned perfectly with the published hamster sequence (NW_004801604.1) (Fig. 8). The conserved Q147R mutation site was also intact between all three sequences. Based on the sequencing result, I designed an sgRNA/Cas9 vector to target the hamster *KCNQ1* exon 2 with the PAM sequence six nucleotides downstream of the Q147R mutation site position.
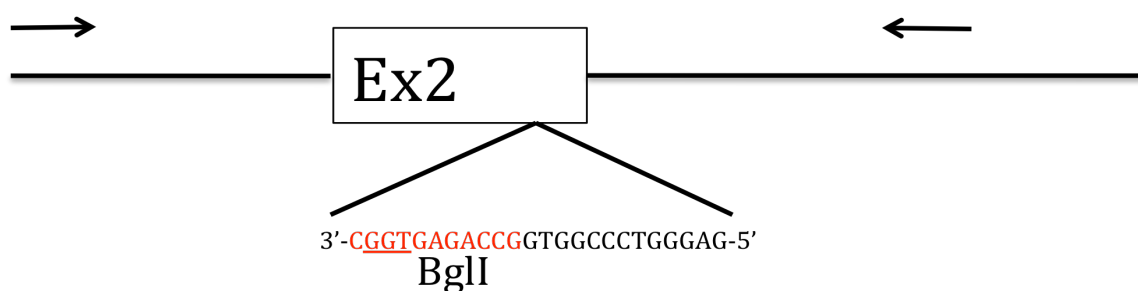

3'-CGGTGAGACCGGTGGCCCTGGGAG-5'
BglI

Fig. 9 Schematic of hamster *KCNQ1* targeting location. PCR primers (arrows) amplify exon 2 and surrounding intron sequence. The target site (PAM underlined) includes a BglI restriction site (red text), which will be used for RFLP analysis.

KCNQ1 Knockout Gene-targeting

As mentioned above, I chose to focus on the DNA sequence that is close to the Q147R mutation site (Fig. 9) by designing and constructing a gRNA template to target it. To test gene-targeting efficiency, I transfected the sgRNA/Cas9-expressing vector targeting hamster exon 2 into BHK cells and conducted RFLP analysis on the transfected cells 48 hours post-transfection.

This CRISPR showed activity ranging from 10-60%, depending on the amount of plasmid DNA used in the transfection. Transfections using 2 µg of plasmid lead to efficiencies of 10-20% (Fig. 10 A). Increasing transfection amount to 4 µg greatly increased efficiency to as high as 60% (Fig. 10 B). Results were further confirmed by SURVEYOR nuclease assay (Fig.

11). Using this assay, indel efficiency was estimated to be about 15%, comparable to the ranges

of efficiency estimated by RFLP.
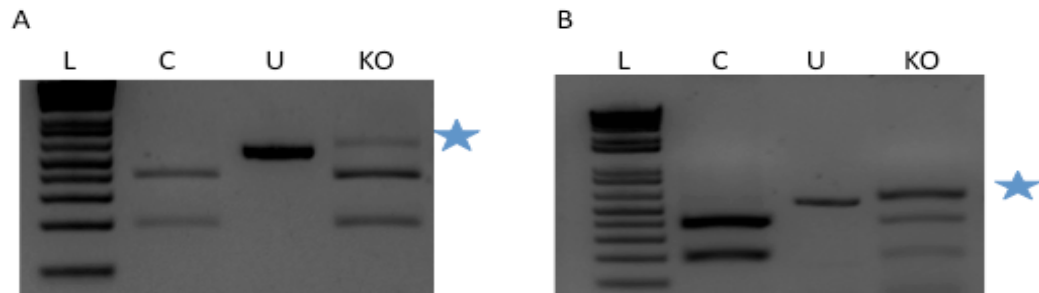
Fig. 10 Indel efficiency is influenced by the amount of sgRNA/Cas9 transfected. Transfecting 2 μg sgRNA/Cas9 plasmid (A) generates a faint band resistant to BglI digest (Starred) with an estimated indel efficiency of 10%. Doubling the sgRNA/Cas9 plasmid amount to 4 μg (B) generates an even brighter band after digest with an indel efficiency of 60%. L=1kb Plus DNA Ladder. C=Control DNA cut with BglI. U=Knockout DNA uncut. KO=Knockout DNA cut with BglI.
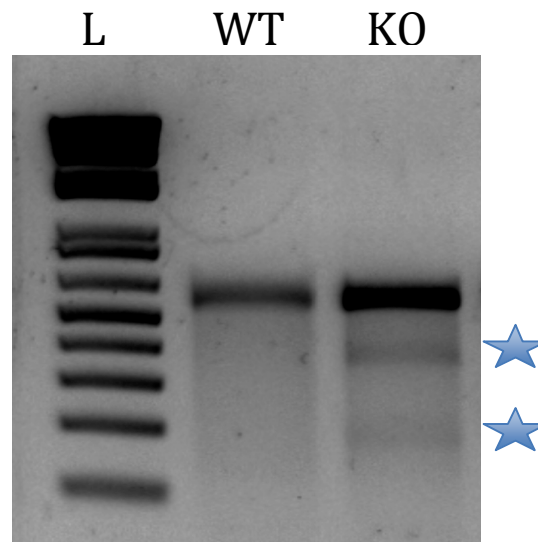
Fig. 11 SURVEYOR assay confirms results from RFLP analysis. The SURVEYOR assay is described in the methods section. DNA transfected with sgRNA/Cas9 (KO) can be cut by SURVEYOR nuclease indicating dihybrid formation containing DNA with indels. SURVEYOR digest products have been starred.

Single-Cell Derived BHK Knockout Cell Line Establishment

I conducted limiting dilutions on the sgRNA/Cas9 transfected BHK cells 48 hours post transfection to establish single cell-derived BHK cell lines. This was done with the following purposes in mind. First, I wanted to characterize the types of mutations that were induced by this sgRNA/Cas9 gene-targeting vector at a single-cell level (as all of the cells from a established cell line derived from a single cell). Second, the targeted cell lines can potentially provide an *in vitro* system for studying the function of *KCNQ1* in a kidney-derived cell type. Third, by analyzing each of the cell lines, I can provide an accurate measurement on the gene-targeting efficiency of this gene-targeting vector to validate the accuracy of the RFLP and the Surveyor nuclease assay. Of the 71 colonies that were screened, 7 contained indels yielding a targeting efficiency of 9.8% (Fig. 12A). These cell lines were established from a population of cells transfected with 2 µg of plasmid. Therefore, the efficiency calculated by colony screening is comparable to the efficiency estimated by bulk cell RFLP analysis.

Sanger sequencing was performed on these cell lines to determine the types of knockout mutations that were introduced. A wide variety of indels were detected in these clones, including 2-nucleotide insertions, 1-nucleotide deletions, and 9-nucleotide deletions, among others (Fig. 12 B, Table 3). All but one of the cell lines was heterozygous, containing one targeted allele. The other colony was homozygous harboring identical 1-nucleotide insertions.

Knock in of the Q147R Point Mutation into the Hamster *KCNQ1* Gene

A single-stranded donor oligonucleotide was designed to introduce two precise single nucleotide substitutions into the exon 2 locus. The first mutation is the previously mentioned A to G substitution leading to the Q147R amino acid conversion. The second mutation is a silent

mutation at the CRISPR PAM sequence, designed to abolish the PAM sequence to prevent

CRISPR/Cas9 from re-cleaving the target site after successful oligo integration (Fig. 13).

Flanking the A to G substitution site and the disrupted PAM mutation is a 5' homologous arm 82

nucleotides long, and a 3' homologous arm 60 nucleotides long. To knock in this A to G mutation

into the hamster genome, I co-transfected the oligo into BHK cells with the exon 2-targeting

sgRNA/Cas9 vector.
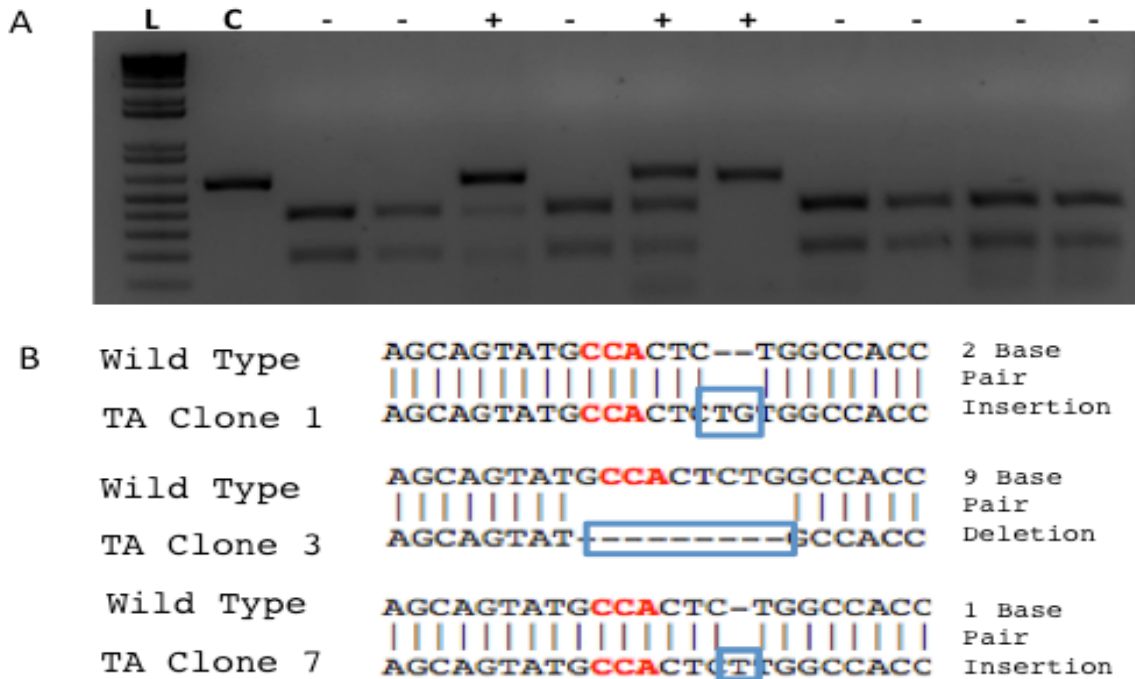
Fig. 12 Screening BHK *KCNQ1* knockout cell lines with RFLP analysis. A) gDNA from BHK KO cell lines was PCR amplified, then digested with BglI. Cell lines containing indels in the target region are resistant to digest (+). C=Control DNA not digested with BglI. B) Sample BHK TA clone sequences aligned to wild type sequences. Different types of knockout alleles were found in these colonies.

After transfection, knockin mutations were examined at the bulk cell level by RFLP

analysis. Successful integration of the donor oligo abolishes a BglI site via the PAM disrupting

substitution (Fig. 13). However, this enzyme site can also be abolished by knockout events

induced by indels making this assay sensitive to both types of targeting events. Using this assay, targeting events were detected (Fig. 14A). Although the ratio of knockout to knockin events can't be determined using this assay, we can conclude that co-transfection of the donor oligo does not hamper the activity of the sgRNA/Cas9 vector.

Table 3 Summary of mutation types observed in TA clones of BHK cell lines Clone 4 was positive for indels by RFLP, but its TA clone was unable to be sequenced.

Clone I.D.	Mutation Type	Genotype
1	2-Nucleotide Insertion	Heterozygous
2	1-Nucleotide Deletion	Heterozygous
3	9-Nucleotide Deletion	Heterozygous
4	N.A.	N.A
5	1-Nucleotide Insertion	Heterozygous
6	6-Nucleotide Deletion	Heterozygous
7	1-Nucleotide Insertion	Homozygous

Unlike in previous RFLP analyses, successful donor oligo integration introduces a BsrBI restriction site at the A to G substitution location, allowing for knockin DNA to be digested by this enzyme (Fig. 13). RFLP analysis for the knockin event showed the expected digest bands, but the intensity of the bands was very faint, indicating that the knockin efficiency was very low. The estimated knockin efficiency was about 6% (Fig. 14 B). Due to the low sensitivity to knockin events of the RFLP and SURVEYOR assays, I decided to develop a new assay capable of detecting lower levels of knockin activity. Towards this goal, I developed a PCR based assay

capable of detecting DNA containing our knockin substitution, but selective against wild type

DNA.
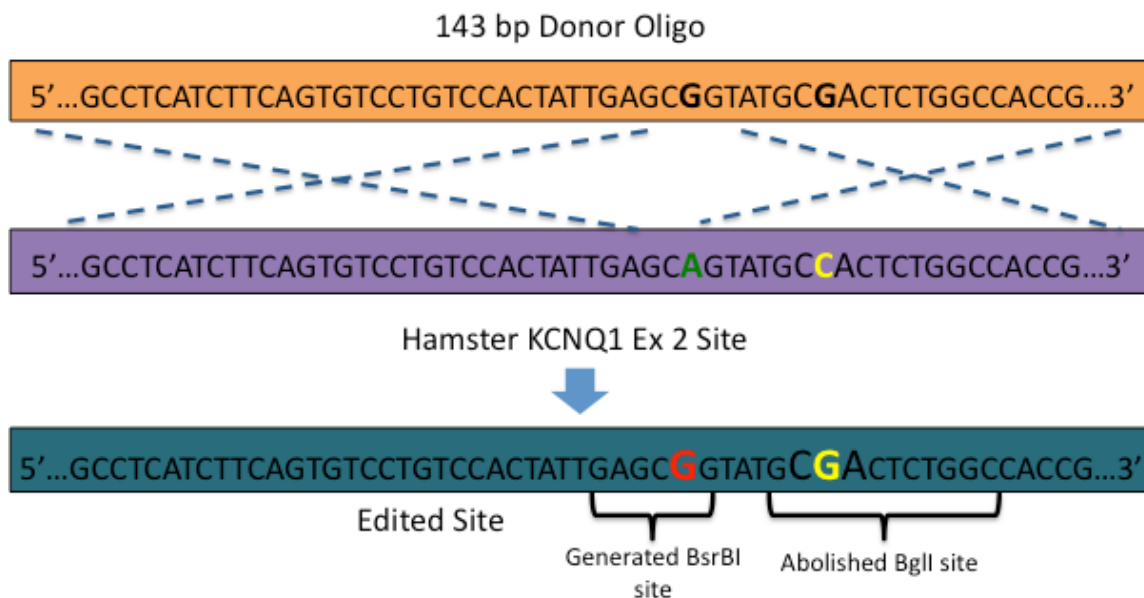
Fig. 13 Schematic of *KCNQ1* knockin using a ssdonor oligonucleotide. When the donor oligo is integrated into the target site, the Q147R A to G substitution (Red) generates a BsrBI site, and the PAM-disrupting mutation (Yellow) abolishes a BglI site. These restriction sites were used for RFLP analysis.
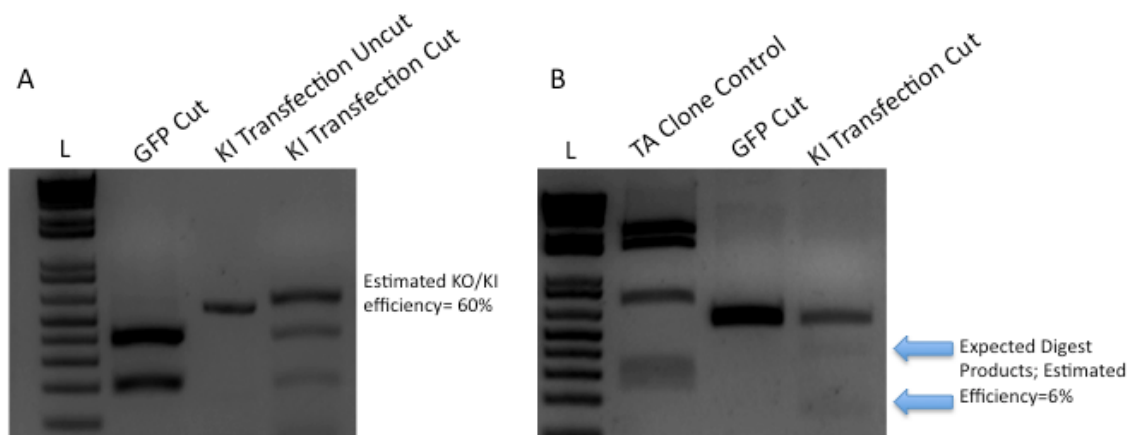
Fig. 14 RFLP analysis of hamster *KCNQ1* knockin. A) BglI digest of knockin DNA left a band resistant to digest indicating that knockout and/or knockin events took place at an efficiency of 60%. B) BsrBI digest of KI DNA produced faint digest products at an efficiency of 6%.

To detect lower levels of targeting efficiency typically found when trying to induce knockin events, a new primer was designed which matched the wild type exon except for the A to G substitution at the 3' clamp. This way the primer matches perfectly with genomic DNA carrying the A to G substitution but does not match the wild type genomic DNA at the 3' end (Fig. 15). Combined with the reverse primer flanking the 3' end of exon 2 (Fig. 9), knockin template DNA is expected to produce a 398 nucleotide PCR product.
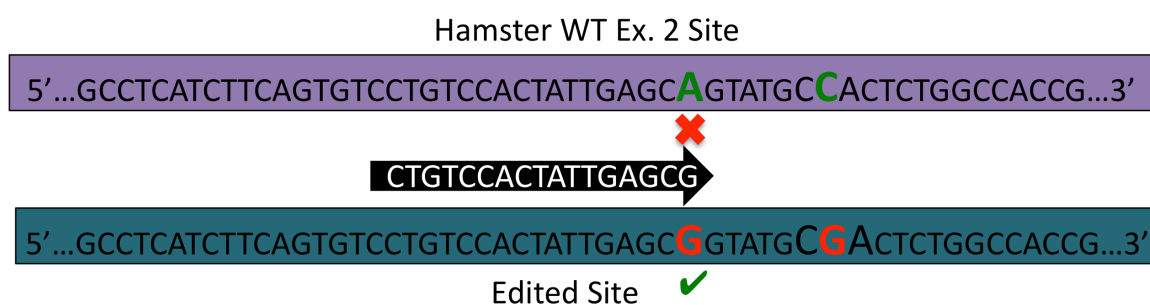
Fig. 15 *KCNQ1* knockin-sensitive PCR primer. The primer's 3' clamp contains the A to G substitution. This primer, paired with the exon2-flanking reverse primer, amplifies knockin gDNA, but is unable to amplify wild type gDNA.

To test the new assay's selectivity towards wild type genomic DNA, different PCR conditions were tested using wild type gDNA as template. A wide range of annealing temperatures was tested to identify the PCR conditions that do not amplify the wild type genomic DNA templates. Under the PCR conditions tested, the primer pair was found to be highly selective against the wild type DNA template as it was unable to generate any PCR product (Fig. 16 A). Next, gDNA transfected with the CRISPR plasmid and donor oligo was used as PCR template for the same primer pair. The expected PCR product was observed at high levels in multiple reactions when the donor oligo was used in the transfection (Fig. 16 B). Sequencing these products confirmed the positive results of the assay by detection of the PAM-disrupting mutation (Fig. 16 C).
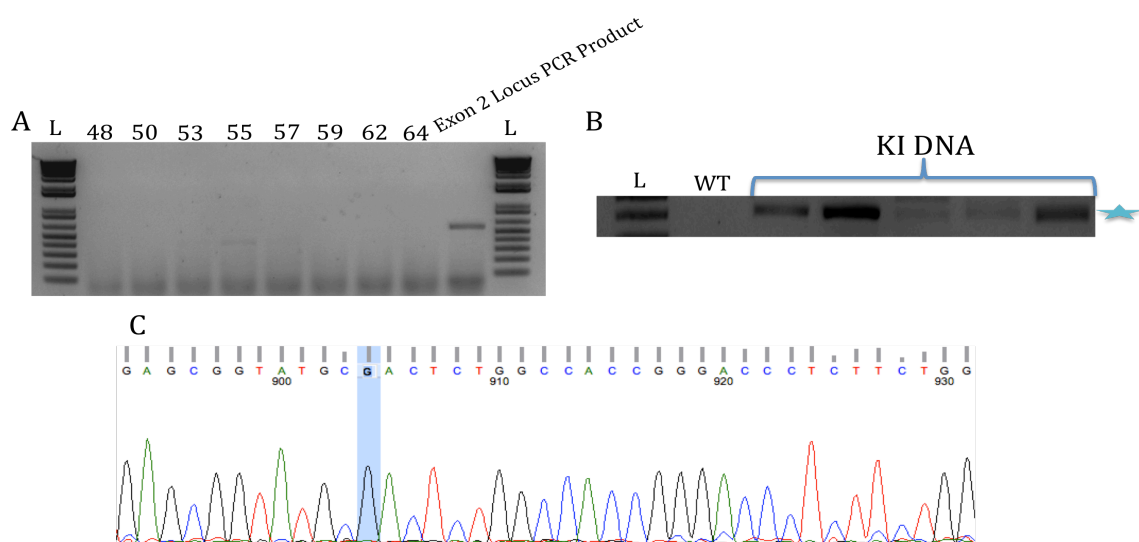
Fig. 16 PCR based assay of *KCNQ1* knockin events. A) Knockin sensitive PCR primers were unable to amplify wild type DNA regardless of what annealing temperature was used. Amplification with the original exon 2 primer pair (Fig. 9) was performed in parallel to control for PCR conditions. B) Multiple samples of knockin transfected gDNA (KI DNA) produced the expected 398 nucleotide PCR product. (star) C) Identification of the PAM-disrupting silent mutation (blue highlight) confirmed the PCR results.

KCNQ1 Knockout/Knockin Hamster Generation

In BHK cells, the CRISPR targeting exon 2 induced indels with efficiencies as high as 60%. Using this same CRISPR with a single-stranded donor oligo, we were also able to detect low levels of knockin events (estimated to be 6% by the RFLP assay). These results gave us confidence to use this CRISPR and donor for generation of live hamsters with *KCNQ1* modifications, both knockouts and gain-of-function point mutation knockins.

In order to generate live animals with *KCNQ1* mutations, hamster embryos were co-microinjected with sgRNA/Cas9 vector and donor oligo into hamster pronuclei. In total, the survival rate of the injected embryos has been 88.5% (Table 4). Injected embryos have been transferred to a total of eight recipients. Unfortunately, none of these litters contained any gene edited pups, but a new round of injections are scheduled to take place in the near future. In the

past our lab has been able to achieve a gene knockout efficiency of 13% using these techniques

in hamsters. Therefore, we expect the next round of injections to produce adequate numbers of

KCNQ1 knockout hamsters with the potential to produce some KNCQ1 knockin animals.

Table 4 Injection and pregnancy table for *KCNQ1* KO/KI hamster generation

Recipient ID	Survival/Injection	Embryo Transfer Number	Date of Birth	Number of Pups Born
1. B15	10/11 (91%)	5/5	11/22/2015	0
2. B19	20/23 (87%)	10/10	11/26/2015	0
3. C31	23/25 (92%)	12/11	11/27/2015	3
4. B25	25/29 (86%)	12/13	11/28/2015	0
5. B12	22/25 (88%)	10/12	12/05/2015	3
6. B27	20/25 (80%)	10/10	12/05/2015	5
Total	154/174 (88.5%)			

Conclusions

Successful characterization of hamster *KCNQ1* exon 2 allowed me to design an

sgRNA/Cas9 expression vector targeting this region to help introduce knockout mutations. It also

allowed for the design of a donor oligo that introduces the AF causing mutation Q147R.

Transfection of the CRISPR produces a high level of mutations in BHK cells. The amount of

plasmid DNA used seemed to have an effect on indel efficiency. Using 2 μg of plasmid produced

efficiencies of about 10%. By doubling this amount, targeting efficiency increased to an upper

bound of 60%. Establishing single-cell derived cell lines from these transfections allowed us to

confirm and characterize the types of indels that were introduced. Many types of the indels that

were found produced premature stop codons leading to loss of gene function (Fig. 17). One

colony was found to be biallelically targeted, leading to a homozygous knockout of *KCNQ1*.
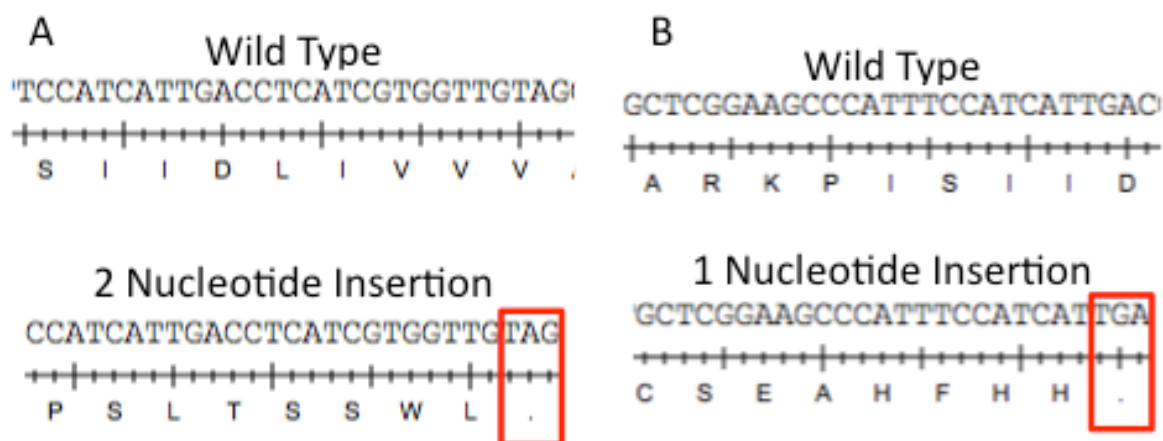
Fig. 17 Hamster *KCNQ1Ex2* knockout mutations lead to premature stop codons. A) The 2-nucleotide insertion produces a premature stop codon (TAG) at position 622. B) The 1-nucleotide insertion produces a premature stop codon (TGA) at position 604. Hamster *KCNQ1* mRNA CDS is 2873 nucleotides long (XM_005064141.2).

We developed a PCR based assay capable of detecting lower levels of knockin events. A

new primer was designed that selects against wild type DNA and those carrying indels and also

selects for DNA containing the A to G substitution coding for the Q147R mutation. The

specificity of this assay was demonstrated by the fact that only genomic DNA isolated from BHK

cells that were co-transfected by the sgRNA/Cas9 vector and the donor oligo can be PCR

amplified to produce the expected 398 nucleotide PCR product, while wild type DNA was unable

to be amplified using this method. The presence of the PAM-disrupting silent mutation was

detected via sequencing, thus confirming the selectivity of the PCR assay.

Based on these results, the *KCNQ1* targeting vector and knockin donor oligo were used for pronuclear injections to produce both *KCNQ1* knockout and gain-of-function point mutation hamsters. Production of these hamsters is currently ongoing. We expect some of these animals to contain loss-of-function mutations with the potential of finding some animals containing the Q147R gain of function mutation. These hamsters will be used as founder animals to establish breeding colonies for producing animal models for LQT1 and AF.

Chapter VI

MERS-COV MODELING USING TRANSGENIC HAMSTERS

h*DPP4* Founder Line Establishment

To create hamsters susceptible to MERS-CoV infection, transgenic hamsters expressing the human *DPP4* (h*DPP4*) gene encoding the cellular receptor for MERS-CoV were produced as part of this thesis project. In the h*DPP4* transgenic hamsters, the h*DPP4* gene was engineered under the control of the keratin 18 (K18) promoter (Fig. 18 A). The K18 promoter used here preferentially drives the expression of the h*DPP4* gene in the epithelial cells of lung, kidney, nervous, and GI tract tissue [141], allowing for preferential expression of the h*DPP4* transgene in tissue infected by MERS-CoV. To facilitate the monitoring of h*DPP4* gene expression in transgenic hamsters, we also linked a GFP reporter gene via the E2A peptide DNA sequence to the 3' end of the coding sequence of the h*DPP4* gene. The E2A DNA sequence allows the h*DPP4* and GFP genes to be transcribed as a single transcript under the K18 promoter, but translated into two independent proteins: the h*DPP4* protein and the GFP protein [142]. Consequently, the expression of the GFP gene faithfully reports the expression of the h*DPP4* gene.

We employed a PiggyBac transposon system for generating h*DPP4* transgenic hamsters. After the construction of the K18-*DPP4*-GFP expression cassette in the pKB12 vector, the expression cassette was subcloned into a PiggyBac vector, pB513B-1, resulting the PBK18-*DPP4*-GFP vector. This vector, along with a plasmid expressing the PiggyBac transposase, was microinjected into the pronuclei of hamster embryos, which were subsequently transferred into day 1 pregnant female recipients for transgenic hamster production. From these recipients, 3 F0 founder animals were born from the 24 pups produced yielding an efficiency of 12.5%.
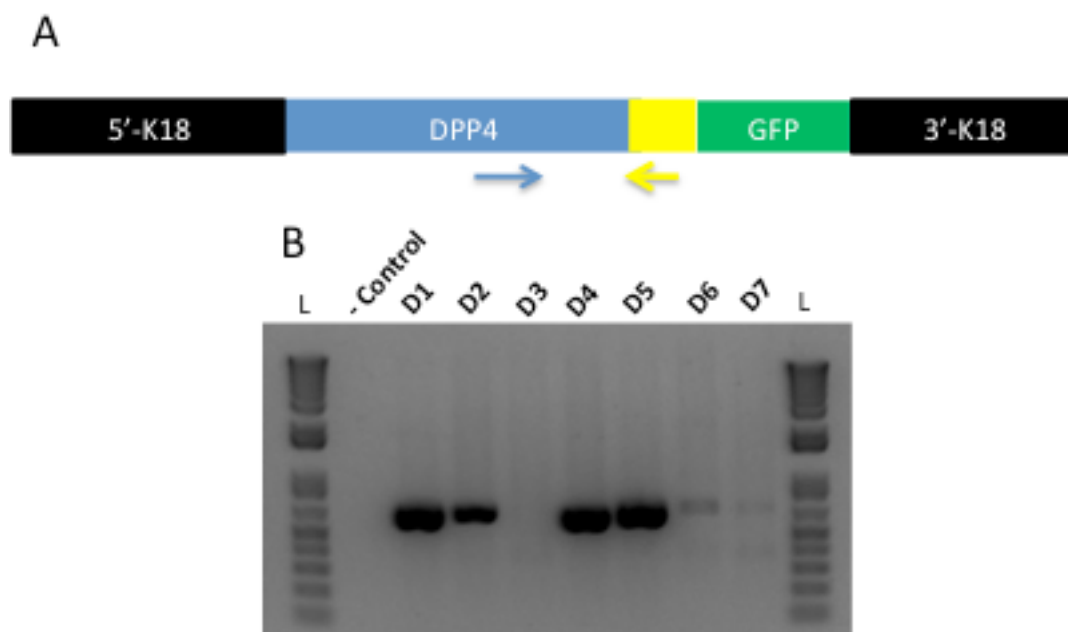
Fig. 18 K18-*DPP4*-GFP cassette is expressed in hamsters. A) The human *DPP4* gene along with GFP and 2A peptide (yellow) have been placed in between 5'- and 3'-K18 promoter segments. Genotyping primers (arrows) are specific for *DPP4* and E2A peptide. B) Representative gel *DPP4* PCR genotyping. *DPP4* positive hamsters produce intense 658 nucleotide PCR products (D1, D2, D4, & D5). The negative control is a PCR reaction using no DNA template.

Genotyping for h*DPP4*-positive F0 founder hamsters, and hamsters deriving from the founder animals was performed via genomic PCR on DNA isolated from toe clippings. We designed the forward primer specific for the h*DPP4* transgene, while the reverse primer begins amplification at the E2A peptide sequence (Fig. 18 A). Hamster DNA carrying the h*DPP4* transgene produces a 368 nucleotide PCR product (Fig. 18 B). Sanger sequencing confirmed the identity of this PCR product. We randomly chose one founder animal to be crossed with wild type animals to establish a h*DPP4* transgenic hamster breeding colony. Crosses between F0 *DPP4*-positive hamsters and wild type animals produced roughly 50% F1 *DPP4*-positive pups, in line with Mendalian inheritance patterns for the h*DPP4* transgene, suggesting a single site integration of the transgene in the hamster genome. To propagate the breeding colony and to provide experimental hamsters for MERS-CoV infection, we further crossed the F1 h*DPP4*-

positive hamsters with wild type hamsters to produce F2 transgenic hamsters, then F2 with

wild type hamsters for F3 transgenic hamsters, and so forth.

Preliminary MERS-CoV Infection Studies

Following propagation of the h*DPP4$^+$* colony, preliminary infection studies were

performed to test for MERS-CoV susceptibility (studies performed by Dr. Dale Barnard).

Lethality was not prominent in these animals, even though all of the h*DPP4* transgenic hamsters

infected by MERS-CoV failed to gain weight throughout 12 days post infection (dpi). Weight

loss was observed in the majority of these animals, with the most dramatic being 10 g in seven

days (Fig. 19). The less severe disease outcomes observed in the infected hamsters, than what was

observed in mouse studies, may reflect different pathogenesis between these species. It is also

possible that the infection dose of virus we used in these experiment was significantly lower than

lethal dose 50% (LD$_{50}$). We are in the process of further characterizing the pathogenesis of

infected hamsters and identifying the LD$_{50}$.

In the *DPP4$^+$* hamsters, virus was targeting lung tissue as is observed in human cases.

Viruses in the range between $10^{2.25}$ and $10^{4.75}$ CCID$_{50}$/0.18 ml were recovered from lung

tissue isolated from the euthanized h*DPP4* transgenic hamsters at 4 dpi (Fig. 20A). The

observation that infected h*DPP4* transgenic hamsters underwent weight loss or failed to gain

weight and that titers of infectious viruses were recovered from the lung tissues of the infected

animals demonstrated that the h*DPP4* transgenic hamsters are susceptible to MERS-CoV

infection. We further revealed that viral RNA was also recovered from h*DPP4$^+$* hamster lungs at

4 dpi, but could not be recovered at day seven (Fig. 20 B). As expected, neither viral titer nor

viral RNA could be detected from wild type littermates of the h*DPP4* transgenic animals.
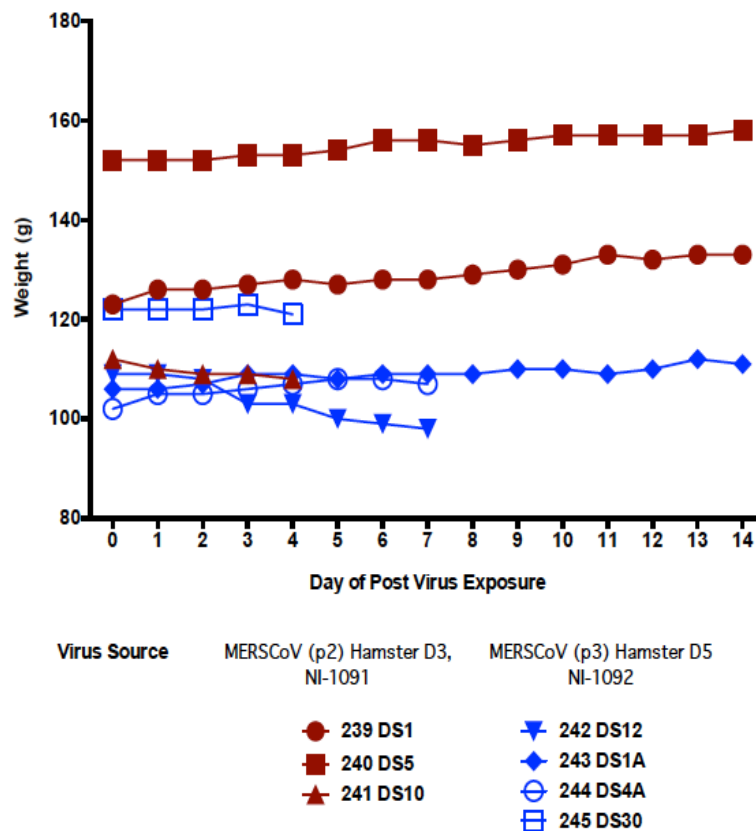
Fig. 19 h*DPP4*⁺ hamsters fail to gain weight or lose weight after MERS-CoV infection. Weight was monitored in these animals up to 14 days post infection. Hamster DS12 had the most dramatic loss of weight, losing 10 grams in 7 days.

Based on these preliminary studies, we concluded that the h*DPP4* transgenic hamsters are susceptible to MERS Co-V. Therefore, we have successfully established a transgenic hamster model for MERS-CoV. As mentioned above, higher doses of virus will be used to test if this hamster model can be used for lethal infection studies. The fact that Viral RNA could only be detected in the lung tissues of the infected h*DPP4* transgenic hamsters at 4 dpi, but not at 7 dpi indicates that infected hamsters can mount an effective immune response to eventually clear the viruses. Type I interferon-mediated innate immunity in Syrian hamsters has been shown to be effective in controlling the infection of many viruses, such as human Adenovirus 5 [119], Ebola virus and dengue virus (our unpublished data).
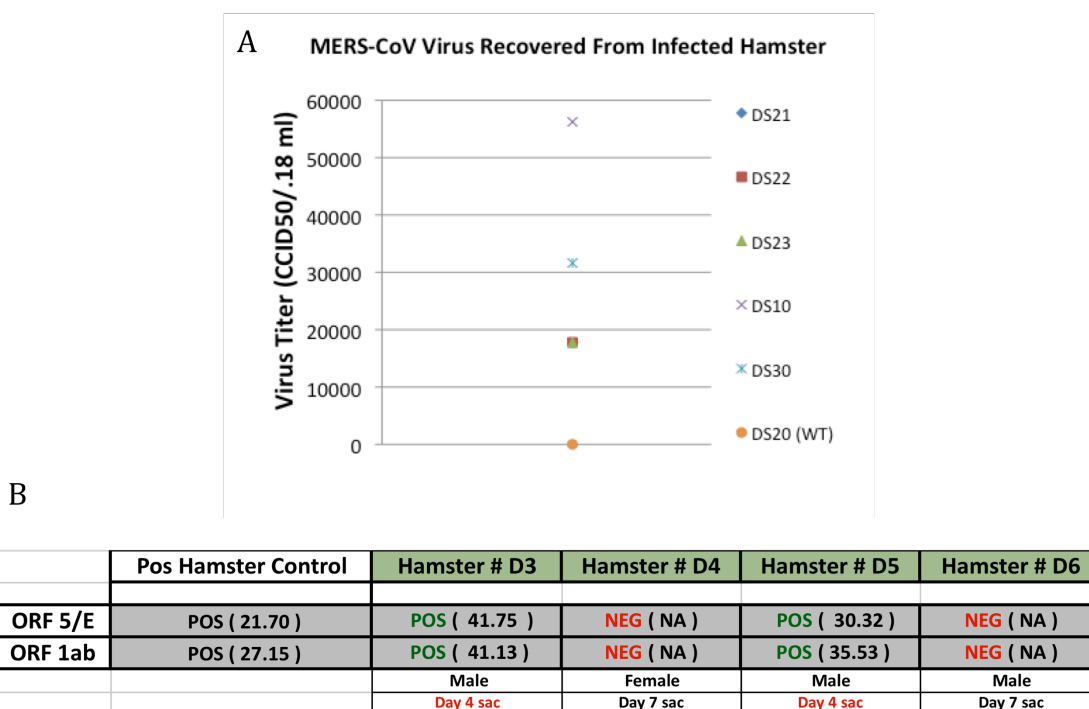
Fig. 20 MERS-CoV could be detected in *DPP4+* hamster lungs 4 days post infection. A) While virus was not detected in the wild type (WT) hamster, all *DPP4⁺* hamsters infected with MERS-CoV had virus ranging between 10^2.25 and 10^4.75 CCID$_{50}$/0.18 ml recovered from their lungs. B) Viral RNA was detected in *DPP4⁺* hamsters on 4, but not 7 days post transfection. Numbers in parentheses are Ct values (Ct values between 20 and 40 indicated a positive test result for MERS-CoV RNA). Positive controls (POS) were from the assay kits.

Creation of h*DPP4* X *STAT2* KO Crosses

Our lab has previously developed a *STAT2* knockout hamster line showing increased susceptibility to viral infection and replication for the viruses that cannot effectively replicate in wild type hamsters [118]. Therefore, we hypothesized that the h*DPP4* transgenic hamsters with a *STAT2* knockout background would lead to a more severe presentation of MERS, and extended viral replication would be enabled. Consequently, in this thesis project, I embarked on crossing the h*DPP4* transgenic hamsters with the *STAT2* knockout heterozygotes (*STAT2⁺/⁻*) to generate h*DPP4* transgenic hamsters with a *STAT2* knockout allele. Five crosses were set up producing fifty-one pups. These pups were genotyped for h*DPP4* and *STAT2* knockout alleles (Table 5).

h*DPP4* was genotyped in the same way discussed above. *STAT2* knockout genotyping was performed via RFLP analysis as described previously [118] (Fig. 21 A). The *STAT2* knockout allele contains a 1-nucleotide insertion that abolishes the restriction site, leaving behind an 869 nucleotide PCR product partially resistant to digest (Fig. 21 B). Six animals from these initial crosses contained the h*DPP4* transgene with a *STAT2* knockout allele (*DPP4*$^{+/-}$; *STAT2*$^{+/-}$).

Table 5 Initial crosses used to generate h*DPP4*$^{+}$; *STAT2*$^{+/-}$ hamsters

Pup I.D.'s	Parents	D.O.B.	Pups with DPP4^{+}; STAT2$^{+/-}$) Genotype
DS1-DS9	F624(STAT2$^{+/-}$)XF2DP01 (DPP4$^{+/-}$)	6/20/15	1/9 (11%)
DS10-DS19	F6I12(STAT2$^{+/-}$)XF2DP01(DPP4$^{+/-}$)	6/25/15	0/10 (0%)
DS20-DS29	F619(STAT2$^{+/-}$)XF2DP01(DPP4$^{+/-}$)	7/2/15	2/10 (20%)
DS30-DS42	F6215(STAT2$^{+/-}$)XF2DP01(DPP4$^{+/-}$)	7/22/15	1/13 (8%)
DS43-DS51	F3D2(DPP4$^{+/-}$)XF6M6(STAT2$^{+/-}$)	7/23/15	2/9 (22%)
		Totals	6/51 (11.7%)

These animals, and other *STAT2* knockout heterozygotes, were crossed with each other to propagate the h*DPP4*$^{+}$; *STAT2*$^{+/-}$ genotype, and to generate *DPP4*$^{+}$ hamsters in a homozygous *STAT2* knockout background (*STAT2*$^{-/-}$). *STAT2* PCR products completely resistant to digest indicated that both *STAT2* alleles in an animal contained the BglII-abolishing insertion (Fig. 21 B). These initial crosses produced six animals with both the h*DPP4* transgene and the *STAT2* homozygous knockout.
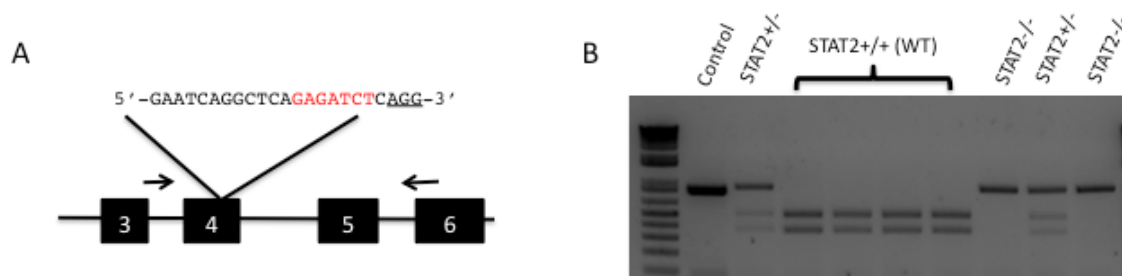
Fig. 21 *STAT2* KO genotyping. A) *STAT2* genomic region was amplified using primers (arrows) flanking the sgRNA target region (PAM underlined). Target region contains a BglII restriction site (red), which was used for RFLP genotyping. B) Representative gel of *STAT2* genotyping for pups generated from *DPP4* X *STAT2*$^{+/-}$ crosses. DNA partially resistant to digest was determined to be *STAT2*$^{+/-}$, while DNA completely resistant to digest was determined to be *STAT2*$^{-/-}$.

Through these breeding efforts, we now have *DPP4*$^{+/-}$; *STAT2*$^{+/-}$ and *DPP4*$^{+/-}$; *STAT2*$^{-/-}$ breeding colonies (Table 6). Breeding efforts are ongoing to increase the numbers of these animals for use in future MERS-CoV infection studies. We suspect that h*DPP4* hamsters in a *STAT2* knockout background will be more susceptible to MERS infection, and/or present with a more severe disease than transgenic hamsters with a wild type background.

Conclusions

Transgenic h*DPP4* founder hamsters were generated via the PiggyBac transposase system and propagated to produce a breeding colony. Preliminary MERS-CoV infection studies were promising as we could detect virus in these animals' lungs both by virus titer and RT-PCR three to four dpi.

MERS-CoV infection was not lethal, but tested animals failed to gain weight or experienced mild weight loss. The weight loss observed in the two previous transgenic mouse models was much more severe, with mice dying as early as 4 dpi, and as late as 13 dpi depending on the mouse model and the dose of virus used [84, 86]. The disease progression of the h*DPP4*

hamsters was most similar to those seen in the Ad5 transposed and humanized *DPP4* mouse

models. In the Ad5 mice, younger animals failed to gain weight while older mice lost weight [82].

Viral infection of humanized mice was not lethal and no weight loss was mentioned [87]. Virus

presence was not tested in other epithelial tissue, nor was tissue pathology tested.

Table 6 h*DPP4* hamsters in the *STAT2* knockout background

Animal I.D.	Sex	DOB	Genotype
DS27	F	7/2/2015	DPP4$^{+/-}$;STAT2$^{+/-}$
DS29	F	7/2/2015	DPP4$^{+/-}$;STAT2$^{+/-}$
DS47	F	7/23/2015	DPP4$^{+/-}$;STAT2$^{+/-}$
DS49	M	7/23/2015	DPP4+/-;STAT2$^{+/-}$
DS2A	F	9/4/2015	DPP4$^{+/-}$;STAT2$^{+/-}$
DS14A	F	10/11/2015	DPP4$^{+/-}$;STAT2$^{+/-}$
DS53	M	8/22/2015	DPP4$^{+/-}$;STAT2-/-
DS56	M	8/22/2015	DPP4$^{+/-}$;STAT2-/-
DS13A	M	10/11/2015	DPP4$^{+/-}$;STAT2-/-
DS15A	F	10/11/2015	DPP4$^{+/-}$;STAT2-/-
DS16A	F	10/24/2015	DPP4$^{+/-}$;STAT2-/-
DS18A	M	10/24/2015	DPP4+/-;STAT2-/-

These preliminary studies show that h*DPP4* hamsters are indeed susceptible to MERS-

CoV infection. However, the disease progression was mild and non-lethal, most closely

resembling the Ad5-h*DPP4* transduced and humanized mouse models. Additionally, virus was

unable to be detected after 4 dpi. We suspect that this mild disease could be due to a robust innate immune system.

Transgenic h*DPP4* hamsters were crossed with *STAT2* knockout hamsters. MERS-susceptible hamsters containing a weakened innate immune system should help to make infection more severe, and allow for virus detection past day 4 pi. Breeding colonies for both h*DPP4*$^{+/-}$; *STAT2*$^{+/-}$ and h*DPP4*$^{+/-}$; *STAT2*$^{-/-}$ genotypes have been established and are being further propagated in order to create sufficient numbers for future infection studies. Future infection studies should expand on the preliminary data, and should include virus detection in other relevant tissues (i.e. nervous and kidney). Tissue pathology should also be examined in future studies. Expanding on preliminary data and adding these other types of studies will allow for a more thorough characterization of our hamster model.

CHAPTER VII

SUMMARY

In this thesis project, progress has been made in the development of goat and hamster models for three deadly diseases. For the goat model, I successfully targeted the *KCNQ1* gene in goat fetal fibroblast cells using the CRISPR/Cas9 genome editing system. Two different loci were targeted. Using the target in exon 2, I established single-cell derived cell lines containing indels that produce premature stop codons. These indels produce functionally abolished *KCNQ1* proteins. Efforts to produce more cell lines like these are ongoing. Additionally, the *KCNQ1* exon 1 locus contains gain-of-function mutation sites known to cause AF. This leaves open the possibility for developing cell lines containing AF inducing mutations with an sgRNA/Cas9-expressing vector designed and ready for use in such experiments. Current and future cell lines will be used as nuclear donors for SCNT in order to produce good animal models for long qt syndrome and atrial fibrillation.

For the development of hamster heart disorder models, I also targeted *KCNQ1*. Again, using the CRISPR/Cas9 genome editing system, the hamster *KCNQ1* exon 2 was successfully targeted and knocked out in BHK cells. Single cell-derived lines were established, not only allowing us to determine specifically what kind of knockout mutations were produced, but also having the potential for future functional studies. Many of these mutations produced frameshift mutations leading to premature stop codons resulting in a non-functional protein.

Using a single-stranded donor oligo along with the exon 2-targeting sgRNA/Cas9 vector, I was also able to induce very low levels of a *KCNQ1* gain-of function mutation. This mutation contains an A to G substitution resulting in the amino acid conversion Q147R, previously reported to cause lone atrial fibrillation. I was able to detect this mutation in BHK cells using a

PCR based assay. In this assay I designed a primer that would amplify DNA containing the Q147R mutation, but not wild type DNA.

The sgRNA/Cas9 targeting vector and the single stranded donor oligonucleotide have been co-injected into pronuclear stage hamster embryos, and transferred to female recipients. The transferred embryos should develop into live animals containing *KCNQ1* knockout mutations, and some may contain the A to G substitution mutation. Although the first round of injections were not successful, another round of injections are scheduled to begin soon. The animals produced should become good animals models for long qt syndrome and atrial fibrillation.

Finally, I have also significantly contributed to the efforts to develop a hamster model of Middle East Respiratory Syndrome. A h*DPP4* transgene harboring a GFP reporter gene was integrated into the hamster genome. Founder animals were expanded, and then used for preliminary MERS-CoV infections. These studies show that h*DPP4* positive hamsters are susceptible to MERS-CoV, but have a mild disease progression similar to two previously generated mouse models [82, 87].

I crossed these h*DPP4* hamsters with *STAT2* knockout hamsters in order to produce a more severe MERS-CoV disease progression in these animals. Two breeding colonies have been successfully established from these crosses. One colony is positive for h*DPP4* and heterozygous for the *STAT2* knockout allele ($STAT2^{+/-}$), and the other is positive for h*DPP4* and homozygous for the *STAT2* knockout ($STAT2^{-/-}$). These colonies will be further propagated and used for more MERS-CoV infection studies in the effort to develop a hamster MERS-CoV model.

In summary, my efforts for this thesis project have laid the foundations for the development of alternative genetic animal models for three deadly diseases with a need for these types of models. Goats generated from the *KCNQ1* knockout cell lines I established should produce unique genetically engineered large animal models for long qt syndrome, with future efforts to be made towards an atrial fibrillation model using cell lines containing the previously

mentioned *KCNQ1* gain-of-function knockin mutation. *KCNQ1* knockout/gain-of-function hamsters made using the sgRNA/Cas9 vector I designed should provide an excellent alternative animal model for LQTS and AF. Lastly the development of the h*DPP4* X *STAT2* knockout hamster colonies will be foundational in the development of a hamster model of MERS-CoV.

REFERENCES

[1] Ericsson, A. C., Crim, M. J., and Franklin, C. L., "A brief history of animal modeling.," *Missouri medicine*, vol. 110, Jan. 2013, pp. 201–5.

[2] Snoy, P. J., "Establishing efficacy of human products using animals: the US food and drug administration's 'animal rule'.," *Veterinary pathology*, vol. 47, Sep. 2010, pp. 774–8.

[3] "eCFR — Code of Federal Regulations," *eCFR — Code of Federal Regulations* Available: http://www.ecfr.gov/cgi-bin/text-idx?sid=8796fb73b71076b76e0cb9d2364774de&mc=true&node=sp21.5.314.i&rgn=div6.

[4] Sharma, R., Lahiri, R., Scollard, D. M., Pena, M., Williams, D. L., Adams, L. B., Figarola, J., and Truman, R. W., "The armadillo: a model for the neuropathy of leprosy and potentially other neurodegenerative diseases.," *Disease models & mechanisms*, vol. 6, Jan. 2013, pp. 19–24.

[5] Truman, R. W., Ebenezer, G. J., Pena, M. T., Sharma, R., Balamayooran, G., Gillingwater, T. H., Scollard, D. M., McArthur, J. C., and Rambukkana, A., "The armadillo as a model for peripheral neuropathy in leprosy.," *ILAR journal / National Research Council, Institute of Laboratory Animal Resources*, vol. 54, Jan. 2014, pp. 304–14.

[6] Cook, N., Jodrell, D. I., and Tuveson, D. A., "Predictive in vivo animal models and translation to clinical trials.," *Drug discovery today*, vol. 17, Mar. 2012, pp. 253–60.

[7] Singh, M., Murriel, C. L., and Johnson, L., "Genetically engineered mouse models: closing the gap between preclinical data and trial outcomes.," *Cancer research*, vol. 72, Jun. 2012, pp. 2695–700.

[8] Wong, P., Cai, H., Borchelt, D., and Price, D., "Genetically engineered mouse models of neurodegenerative diseases," *Nature Neuroscience*, vol. 5, 2002.

[9] Doetschman, T., and Azhar, M., "Cardiac-specific inducible and conditional gene targeting in mice.," *Circulation research*, vol. 110, May 2012, pp. 1498–512.

[10] Cook, N., Jodrell, D. I., and Tuveson, D. A., "Predictive in vivo animal models and translation to clinical trials.," *Drug discovery today*, vol. 17, Mar. 2012, pp. 253–60.

[11] Roberts, T. G., Goulart, B. H., Squitieri, L., Stallings, S. C., Halpern, E. F., Chabner, B. A., Gazelle, G. S., Finkelstein, S. N., and Clark, J. W., "Trends in the risks and benefits to patients with cancer participating in phase 1 clinical trials.,"*JAMA*, vol. 292, Nov. 2004, pp. 2130–40.

[12] Srivastava, R., "Evaluation of anti-atherosclerotic activities of PPAR-α, PPAR-γ, and LXR agonists in hyperlipidemic atherosclerosis-susceptible F(1)B hamsters.," *Atherosclerosis*, vol. 214, 2010, pp. 86–93.

[13] Kannel, W. B., and Benjamin, E. J., "Current perceptions of the epidemiology of atrial fibrillation.," *Cardiology clinics*, vol. 27, Feb. 2009, pp. 13–24, vii.

[14] Thijssen, V. L., Ausma, J., and Borgers, M., "Structural remodelling during chronic atrial fibrillation: act of programmed cell survival.," *Cardiovascular research*, vol. 52, Oct. 2001, pp. 14–24.

[15] Potpara, T., and Lip, G., "Lone atrial fibrillation – an overview," *International Journal of Clinical Practice*, vol. 68, 2014, pp. 418–433.

[16] Nattel, S., Guasch, E., Savelieva, I., Cosio, F. G., Valverde, I., Halperin, J. L., Conroy, J. M., Al-Khatib, S. M., Hess, P. L., Kirchhof, P., Bono, J. De, Lip, G. Y., Banerjee, A., Ruskin, J., Blendea, D., and Camm, A. J., "Early management of atrial fibrillation to prevent cardiovascular complications.," *European heart journal*, vol. 35, Jun. 2014, pp. 1448–56.

[17] Nattel, S, Shiroshita-Takeshita, A, and Brundel, B., "Mechanisms of atrial fibrillation: lessons from animal models," *Progress in ...*, 2005.

[18] Wijffels, Kirchhof, Dorland, and Allessie, "Atrial Fibrillation Begets Atrial Fibrillation : A Study in Awake Chronically Instrumented Goats," *Circulation*, vol. 92, 1995.

[19] Mills, L. C., Gow, R. M., Myers, K., Kantoch, M. J., Gross, G. J., Fournier, A., and Sanatani, S., "Lone atrial fibrillation in the pediatric population.," *The Canadian journal of cardiology*, vol. 29, Oct. 2013, pp. 1227–33.

[20] Benjamin, E., Wolf, P., D'Agostino, R., Silbershatz, H., Kannel, W., and Levy, D., "Impact of Atrial Fibrillation on the Risk of Death The Framingham Heart Study,"*Circulation*, vol. 98, 1998, pp. 946–952.

[21] Wolf, P., Abbott, R., and Kannel, W., "Atrial fibrillation as an independent risk factor for stroke: the Framingham Study.," *Stroke*, vol. 22, 1991, pp. 983–988.

[22] Wang, T., Larson, M., Levy, D., Vasan, R., Leip, E., Wolf, P., D'Agostino, R., Murabito, J., Kannel, W., and Benjamin, E., "Temporal relations of atrial fibrillation and congestive heart failure and their joint influence on mortality: the Framingham Heart Study.,"*Circulation*, vol. 107, 2003, pp. 2920–5.

[23] Coyne, K., Paramore, C., Grandy, S., Mercader, M., Reynolds, M., and Zimetbaum, P., "Assessing the Direct Costs of Treating Nonvalvular Atrial Fibrillation in the United States," *Value in Health*, vol. 9, 2006, pp. 348–356.

[24] Stewart, S., Murphy, N., Murphy, N., Walker, A., McGuire, A., and McMurray, J., "Cost of an emerging epidemic: an economic analysis of atrial fibrillation in the UK," *Heart*, vol. 90, 2004, pp. 286–292.

[25] Crotti, L., Celano, G., Dagradi, F., and Schwartz, P., "Congenital long QT syndrome," *Orphanet Journal of Rare Diseases*, vol. 3, 2008, p. 18.

[26] Tester, D. J., and Ackerman, M. J., "Genetics of long QT syndrome.,"*Methodist DeBakey cardiovascular journal*, vol. 10, Jan. 2014, pp. 29–33.

[27] Schwartz, P., Crotti, L., and Insolia, R., "Long-QT syndrome: from genetics to management.," *Circulation. Arrhythmia and electrophysiology*, vol. 5, 2012, pp. 868–77.

[28] Locati, E. H., Zareba, W., Moss, A. J., Schwartz, P. J., Vincent, G. M., Lehmann, M. H., Towbin, J. A., Priori, S. G., Napolitano, C., Robinson, J. L., Andrews, M., Timothy, K., and Hall, W. J., "Age- and sex-related differences in clinical manifestations in patients with congenital long-QT syndrome: findings from the International LQTS Registry.," *Circulation*, vol. 97, Jun. 1998, pp. 2237–44.

[29] Zareba, W., Moss, A. J., Locati, E. H., Lehmann, M. H., Peterson, D. R., Hall, W. J., Schwartz, P. J., Vincent, G. M., Priori, S. G., Benhorin, J., Towbin, J. A., Robinson, J. L., Andrews, M. L., Napolitano, C., Timothy, K., Zhang, L., and Medina, A., "Modulating effects of age and gender on the clinical course of long QT syndrome by genotype.," *Journal of the American College of Cardiology*, vol. 42, Jul. 2003, pp. 103–9.

[30] Kannankeril, P., Roden, D. M., and Darbar, D., "Drug-induced long QT syndrome.,"*Pharmacological reviews*, vol. 62, Dec. 2010, pp. 760–81.

[31] Dvir, M., Peretz, A., Haitin, Y., and Attali, B., "Recent molecular insights from mutated IKS channels in cardiac arrhythmia.," *Current opinion in pharmacology*, vol. 15, Apr. 2014, pp. 74–82.

[32] Yu, F. H., Yarov-Yarovoy, V., Gutman, G. A., and Catterall, W. A., "Overview of molecular relationships in the voltage-gated ion channel superfamily.,"*Pharmacological reviews*, vol. 57, Dec. 2005, pp. 387–95.

[33] Jost, N., Papp, J. G., and Varró, A., "Slow delayed rectifier potassium current (IKs) and the repolarization reserve.," *Annals of noninvasive electrocardiology : the official journal of the International Society for Holter and Noninvasive Electrocardiology, Inc*, vol. 12, Jan. 2007, pp. 64–78.

[34] Grizel, A. V., Glukhov, G. S., and Sokolova, O. S., "Mechanisms of activation of voltage-gated potassium channels.," *Acta naturae*, vol. 6, Oct. 2014, pp. 10–26.

[35] Chen, Y.-H., Xu, S.-J., Bendahhou, S., Wang, X.-L., Wang, Y., Xu, W.-Y., Jin, H.-W., Sun, H., Su, X.-Y., Zhuang, Q.-N., Yang, Y.-Q., Li, Y.-B., Liu, Y., Xu, H.-J., Li, X.-F., Ma, N., Mou, C.-P., Chen, Z., Barhanin, J., and Huang, W., "KCNQ1 Gain-of-Function Mutation in Familial Atrial Fibrillation," *Science*, vol. 299, 2003, p. 251254.

[36] Hong, K., Piper, D., Diaz-Valdecantos, A., Brugada, J., Oliva, A., Burashnikov, E., Santos-de-Soto, J., Grueso-Montero, J., Diaz-Enfante, E., Brugada, P., Sachse, F., Sanguinetti, M., and Brugada, R., "De novo KCNQ1 mutation responsible for atrial fibrillation and short QT syndrome in utero," *Cardiovascular Research*, vol. 68, 2005, p. 433440.

[37] Restier, L., Cheng, L., and Sanguinetti, M. C., "Mechanisms by which atrial fibrillation-associated mutations in the S1 domain of KCNQ1 slow deactivation of IKs channels.," *The Journal of physiology*, vol. 586, Sep. 2008, pp. 4179–91.

[38] Lundby, A., Ravn, L. S., Svendsen, J. H., Olesen, S.-P. P., and Schmitt, N., "KCNQ1 mutation Q147R is associated with atrial fibrillation and prolonged QT interval.," *Heart rhythm : the official journal of the Heart Rhythm Society*, vol. 4, Dec. 2007, pp. 1532–41.

[39] Wang, Q., Curran, M. E., Splawski, I., Burn, T. C., Millholland, J. M., VanRaay, T. J., Shen, J., Timothy, K. W., Vincent, G. M., Jager, T. de, Schwartz, P. J., Toubin, J. A., Moss, A. J., Atkinson, D. L., Landes, G. M., Connors, T. D., and Keating, M. T., "Positional cloning of a novel potassium channel gene: KVLQT1 mutations cause cardiac arrhythmias.,"*Nature genetics*, vol. 12, Jan. 1996, pp. 17–23.

[40] Keating, M., and Sanguinetti, M., "Molecular and Cellular Mechanisms of Cardiac Arrhythmias," *Cell*, vol. 104, 2001.

[41] Lee, M. P., Hu, R. J., Johnson, L. A., and Feinberg, A. P., "Human KVLQT1 gene shows tissue-specific imprinting and encompasses Beckwith-Wiedemann syndrome chromosomal rearrangements.," *Nature genetics*, vol. 15, Feb. 1997, pp. 181–5.

[42] Gurrieri, F., Zollino, M., Oliva, A., Pascali, V., Orteschi, D., Pietrobono, R., Camporeale, A., Coll Vidal, M., Partemi, S., Brugada, R., Bellocci, F., and Neri, G., "Mild Beckwith-Wiedemann and severe long-QT syndrome due to deletion of the imprinting center 2 on chromosome 11p.," *European journal of human genetics : EJHG*, vol. 21, Sep. 2013, pp. 965–9.

[43] Nattel, S, Shiroshita-Takeshita, A, and Brundel, B., "Mechanisms of atrial fibrillation: lessons from animal models,"*Progress in ...*, 2005.

[44] Ortiz, J, Niwano, S, Abe, H, Rudy, Y, and Johnson, NJ, "Mapping the conversion of atrial flutter to atrial fibrillation and atrial fibrillation to atrial flutter. Insights into mechanisms.,"*Circulation ...*, 1994.

[45] Nishida, K., Michael, G., Dobrev, D., and Nattel, S., "Animal models for atrial fibrillation: clinical insights and scientific opportunities.," *Europace : European pacing, arrhythmias, and cardiac electrophysiology : journal of the working groups on cardiac pacing, arrhythmias, and cardiac cellular electrophysiology of the European Society of Cardiology*, vol. 12, Feb. 2010, pp. 160–72.

[46] Li, D, Fareh, S, Leung, TK, and Nattel, S, "Promotion of atrial fibrillation by heart failure in dogs atrial remodeling of a different sort," *Circulation*, 1999.

[47] Marx, SO, Kurokawa, J, Reiken, S, and Motoike, H, "Requirement of a macromolecular signaling complex for β adrenergic receptor modulation of the KCNQ1-KCNE1 potassium channel," *Science*, 2002.

[48] Sampson, K. J., Terrenoire, C., Cervantes, D. O., Kaba, R. A., Peters, N. S., and Kass, R. S., "Adrenergic regulation of a key cardiac potassium channel can contribute to atrial fibrillation: evidence from an I Ks transgenic mouse." *The Journal of physiology*, vol. 586, Jan. 2008, pp. 627–37.

[49] Kupershmidt, S., Yang, T., Anderson, M. E., Wessels, A., Niswender, K. D., Magnuson, M. A., and Roden, D. M., "Replacement by homologous recombination of the minK gene with lacZ reveals restriction of minK expression to the mouse cardiac conduction system.," *Circulation research*, vol. 84, Feb. 1999, pp. 146–52.

[50] Temple, J., Frias, P., Rottman, J., Yang, T., Wu, Y., Verheijck, E. E., Zhang, W., Siprachanh, C., Kanki, H., Atkinson, J. B., King, P., Anderson, M. E., Kupershmidt, S., and Roden, D. M., "Atrial fibrillation in KCNE1-null mice." *Circulation research*, vol. 97, Jul. 2005, pp. 62–9.

[51] Olgin, JE, and Verheule, S, "Transgenic and knockout mouse models of atrial arrhythmias,"*Cardiovascular research*, 2002.

[52] Verheule, S, Sato, T, Everett, T, and Engle, SK, "Increased vulnerability to atrial fibrillation in transgenic mice with selective atrial fibrosis caused by overexpression of TGF-β1," *Circulation …*, 2004.

[53] Nerbonne, J. M., "Studying cardiac arrhythmias in the mouse--a reasonable model for probing mechanisms?," *Trends in cardiovascular medicine*, vol. 14, Apr. 2004, pp. 83–93.

[54] Salama, G., and London, B., "Mouse models of long QT syndrome.," *The Journal of physiology*, vol. 578, Jan. 2007, pp. 43–53.

[55] Carlsson, L., "In vitro and in vivo models for testing arrhythmogenesis in drugs.,"*Journal of internal medicine*, vol. 259, Jan. 2006, pp. 70–80.

[56] Kannankeril, P., Roden, D. M., and Darbar, D., "Drug-induced long QT syndrome.," *Pharmacological reviews*, vol. 62, Dec. 2010, pp. 760–81.

[57] Morey, T. E., Martynyuk, A. E., Napolitano, C. A., Raatikainen, M. J., Guyton, T. S., and Dennis, D. M., "Ionic basis of the differential effects of intravenous anesthetics on erythromycin-induced prolongation of ventricular repolarization in the guinea pig heart.," *Anesthesiology*, vol. 87, Nov. 1997, pp. 1172–81.

[58] Vos, M. A., Verduyn, S. C., Gorgels, A. P., Lipcsei, G. C., and Wellens, H. J., "Reproducible induction of early afterdepolarizations and torsade de pointes arrhythmias by d-sotalol and pacing in dogs with chronic atrioventricular block.,"*Circulation*, vol. 91, Feb. 1995, pp. 864–72.

[59] Lee, M. P., Ravenel, J. D., Hu, R. J., Lustig, L. R., Tomaselli, G., Berger, R. D., Brandenburg, S. A., Litzi, T. J., Bunton, T. E., Limb, C., Francis, H., Gorelikow, M., Gu, H., Washington, K., Argani, P., Goldenring, J. R., Coffey, R. J., and Feinberg, A. P., "Targeted disruption of the Kvlqt1 gene causes deafness and gastric hyperplasia in mice.," *The Journal of clinical investigation*, vol. 106, Dec. 2000, pp. 1447–55.

[60] Casimiro, M. C., Knollmann, B. C., Ebert, S. N., Vary, J. C., Greene, A. E., Franz, M. R., Grinberg, A., Huang, S. P., and Pfeifer, K., "Targeted disruption of the Kcnq1 gene produces a mouse model of Jervell and Lange-Nielsen Syndrome.," *Proceedings of the National Academy of Sciences of the United States of America*, vol. 98, Feb. 2001, pp. 2526–31.

[61] Takagi, T., Nishio, H., Yagi, T., Kuwahara, M., Tsubone, H., Tanigawa, N., and Suzuki, K., "Phenotypic analysis of vertigo 2 Jackson mice with a Kcnq1 potassium channel mutation.," *Experimental animals / Japanese Association for Laboratory Animal Science*, vol. 56, Jul. 2007, pp. 295–300.

[62] Wessels, A., and Sedmera, D., "Developmental anatomy of the heart: a tale of mice and man.," *Physiological genomics*, vol. 15, Nov. 2003, pp. 165–76.

[63] Vermeulen, J. T., Mcguire, M. A., Opthof, T., Coronel, R., Bakker, J. M. T. D., Klopping, C., and Janse, M. J., "Triggered activity and automaticity in ventricular trabeculae of failing human and rabbit hearts," Cardiovascular Research, 1994, pp. 1547–1554.

[64] Brunner, M., Peng, X., Liu, G. X., Ren, X.-Q. Q., Ziv, O., Choi, B.-R. R., Mathur, R., Hajjiri, M., Odening, K. E., Steinberg, E., Folco, E. J., Pringa, E., Centracchio, J., Macharzina, R. R., Donahay, T., Schofield, L., Rana, N., Kirk, M., Mitchell, G. F., Poppas, A., Zehender, M., and Koren, G., "Mechanisms of cardiac arrhythmias and sudden death in transgenic rabbits with long QT syndrome." *The Journal of clinical investigation*, vol. 118, Jun. 2008, pp. 2246–59.

[65] Zaki, A. M., Boheemen, S. van, Bestebroer, T. M., Osterhaus, A. D., and Fouchier, R. A., "Isolation of a novel coronavirus from a man with pneumonia in Saudi Arabia.," *The New England journal of medicine*, vol. 367, Nov. 2012, pp. 1814–20.

[66] Perlman, "The Middle East Respiratory Syndrome--How Worried Should We Be?,"*mBio*, vol. 4, 2013, pp. e00531–13e00531–13.

[67] Banik, G. R., Khandaker, G., and Rashid, H., "Middle East Respiratory Syndrome Coronavirus 'MERS-CoV': Current Knowledge Gaps.," *Paediatric respiratory reviews*, Apr. 2015.

[68] Memish, Z. A., Al-Tawfiq, J. A., Assiri, A., AlRabiah, F. A., Hajjar, S., Albarrak, A., Flemban, H., Alhakeem, R. F., Makhdoom, H. Q., and Alsubaie, S., "Middle East respiratory syndrome coronavirus disease in children," *The Pediatric infectious disease journal*, vol. 33, 2014, pp. 904–906.

[69] "Middle East respiratory syndrome coronavirus (MERS-CoV)," *World Health Organization* Available: http://www.who.int/emergencies/mers-cov/en/.

[70] Cheng, V. C. C., Chan, J. F., To, K. K., and Yuen, K. Y., "Clinical management and infection control of SARS: lessons learned.,"*Antiviral research*, vol. 100, Nov. 2013, pp. 407–19.

[71] "Middle East Respiratory Syndrome Coronavirus Outbreak in the Republic of Korea, 2015.," *Osong public health and research perspectives*, vol. 6, Aug. 2015, pp. 269–78.

[72] Ying, T, Li, H, Lu, L, Dimitrov, DS, and Jiang, S, "Development of human neutralizing monoclonal antibodies for prevention and therapy of MERS-CoV infections," *Microbes and Infection*, 2015.

[73] Raj, V. S., Mou, H., Smits, S. L., Dekkers, D. H., Müller, M. A., Dijkman, R., Muth, D., Demmers, J. A. A., Zaki, A., Fouchier, R. A., Thiel, V., Drosten, C., Rottier, P. J., Osterhaus, A. D., Bosch, B. J., and Haagmans, B. L., "Dipeptidyl peptidase 4 is a functional receptor for the emerging human coronavirus-EMC.," *Nature*, vol. 495, Mar. 2013, pp. 251–4.

[74] Chen, Y., Rajashankar, K., Yang, Y., Agnihothram, S., Liu, C., Lin, Y.-L., Baric, R., and Li, F., "Crystal structure of the receptor-binding domain from newly emerged Middle East respiratory syndrome coronavirus.,"*Journal of virology*, vol. 87, 2013.

[75] Lu, G., Hu, Y., Wang, Q., Qi, J., Gao, F., Li, Y., Zhang, Y., Zhang, W., Yuan, Y., Bao, J., Zhang, B., Shi, Y., Yan, J., and Gao, G., "Molecular basis of binding between novel human coronavirus MERS-CoV and its receptor CD26," *Nature*, vol. 500, 2013, pp. 227–231.

[76] Wang, N., Shi, X., Jiang, L., Zhang, S., Wang, D., Tong, P., Guo, D., Fu, L., Cui, Y., Liu, X., Arledge, K., Chen, Y.-H., Zhang, L., and Wang, X., "Structure of MERS-CoV spike receptor-binding domain complexed with human receptor DPP4," *Cell Research*, vol. 23, 2013, pp. 986–993.

[77] Doremalen, N. van, Miazgowicz, K. L., Milne-Price, S., Bushmaker, T., Robertson, S., Scott, D., Kinne, J., McLellan, J. S., Zhu, J., and Munster, V. J., "Host species restriction of Middle East respiratory syndrome coronavirus through its receptor, dipeptidyl peptidase 4.,"*Journal of virology*, vol. 88, Aug. 2014, pp. 9220–32.

[78] Wit, E. de, Rasmussen, A. L., Falzarano, D., Bushmaker, T., Feldmann, F., Brining, D. L., Fischer, E. R., Martellaro, C., Okumura, A., Chang, J., Scott, D., Benecke, A. G., Katze, M. G., Feldmann, H., and Munster, V. J., "Middle East respiratory syndrome coronavirus (MERS-CoV) causes transient lower respiratory tract infection in rhesus macaques.," *Proceedings of the National Academy of Sciences of the United States of America*, vol. 110, Oct. 2013, pp. 16598–603.

[79] Yao, Y., Bao, L., Deng, W., Xu, L., Li, F., Lv, Q., Yu, P., Chen, T., Xu, Y., Zhu, H., Yuan, J., Gu, S., Wei, Q., Chen, H., Yuen, K.-Y. Y., and Qin, C., "An animal model of MERS produced by infection of rhesus macaques with MERS coronavirus.," *The Journal of infectious diseases*, vol. 209, Jan. 2014, pp. 236–42.

[80] Falzarano, D., Wit, E. de, Feldmann, F., Rasmussen, A. L., Okumura, A., Peng, X., Thomas, M. J., Doremalen, N. van, Haddock, E., Nagy, L., LaCasse, R., Liu, T., Zhu, J., McLellan, J. S., Scott, D. P., Katze, M. G., Feldmann, H., and Munster, V. J., "Infection with MERS-CoV causes lethal pneumonia in the common marmoset.," *PLoS pathogens*, vol. 10, Aug. 2014, p. e1004250.

[81] Johnson, R. F., Via, L. E., Kumar, M. R., Cornish, J. P., Yellayi, S., Huzella, L., Postnikova, E., Oberlander, N., Bartos, C., Ork, B. L., Mazur, S., Allan, C., Holbrook, M. R., Solomon, J., Johnson, J. C., Pickel, J., Hensley, L. E., and Jahrling, P. B., "Intratracheal exposure of common marmosets to MERS-CoV Jordan-n3/2012 or MERS-CoV EMC/2012 isolates does not result in lethal disease.," *Virology*, vol. 485, Nov. 2015, pp. 422–30.

[82] Zhao, J., Li, K., Wohlford-Lenane, C., Agnihothram, S., Fett, C., Zhao, J., Gale, M., Baric, R., Enjuanes, L., Gallagher, T., McCray, P., and Perlman, S., "Rapid generation of a mouse model for Middle East respiratory syndrome," *Proceedings of the National Academy of Sciences*, vol. 111, 2014, pp. 4970–4975.

[83] Agrawal, A. S., Garron, T., Tao, X., Peng, B.-H. H., Wakamiya, M., Chan, T.-S. S., Couch, R. B., and Tseng, C.-T. K. T., "Generation of a transgenic mouse model of Middle East respiratory syndrome coronavirus infection and disease.," *Journal of virology*, vol. 89, Apr. 2015, pp. 3659–70.

[84] Tao, X., Garron, T., Agrawal, A., Algaissi, A., Peng, B.-H., Wakamiya, M., Chan, T.-S., Lu, L., Du, L., Jiang, S., Couch, R., and Tseng, C.-T., "Characterization and Demonstration of value of a Lethal Mouse Model of Middle East Respiratory Syndrome Coronavirus Infection and Disease," *Journal of Virology*, 2015, pp. JVI.02009–15.

[85] Arabi, YM, Harthi, A, Hussein, J, Bouchama, A, and Johani, S, "Severe neurologic syndrome associated with Middle East respiratory syndrome corona virus (MERS-CoV)," *Infection*, 2015.

[86] Li, K., Wohlford-Lenane, C., Perlman, S., Zhao, J., Jewell, A. K., Reznikov, L. R., Gibson-Corley, K. N., Meyerholz, D. K., and McCray, P. B., "Middle East Respiratory Syndrome Coronavirus Causes Multiple Organ Damage and Lethal Disease in Mice Transgenic for Human Dipeptidyl Peptidase 4.," *The Journal of infectious diseases*, Oct. 2015.

[87] Pascal, K. E., Coleman, C. M., Mujica, A. O., Kamat, V., Badithe, A., Fairhurst, J., Hunt, C., Strein, J., Berrebi, A., Sisk, J. M., Matthews, K. L., Babb, R., Chen, G., Lai, K.-M. V. M., Huang, T. T., Olson, W., Yancopoulos, G. D., Stahl, N., Frieman, M. B., and Kyratsous, C. A., "Pre- and postexposure efficacy of fully human antibodies against Spike protein in a novel humanized mouse model of MERS-CoV infection.," *Proceedings of the National Academy of Sciences of the United States of America*, vol. 112, Jul. 2015, pp. 8738–43.

[88] Seok, J., Warren, H. S., Cuenca, A. G., Mindrinos, M. N., Baker, H. V., Xu, W., Richards, D. R., McDonald-Smith, G. P., Gao, H., Hennessy, L., Finnerty, C. C., López, C. M., Honari, S., Moore, E. E., Minei, J. P., Cuschieri, J., Bankey, P. E., Johnson, J. L., Sperry, J., Nathens, A. B., Billiar, T. R., West, M. A., Jeschke, M. G., Klein, M. B., Gamelli, R. L., Gibran, N. S., Brownstein, B. H., Miller-Graziano, C., Calvano, S. E., Mason, P. H., Cobb, J. P., Rahme, L. G., Lowry, S. F., Maier, R. V., Moldawer, L. L., Herndon, D. N., Davis, R. W., Xiao, W., and Tompkins, R. G., "Genomic responses in mouse models poorly mimic human inflammatory diseases.," *Proceedings of the National Academy of Sciences of the United States of America*, vol. 110, Feb. 2013, pp. 3507–12.

[89] Pearce, A. I., Richards, R. G., Milz, S., Schneider, E., and Pearce, S. G., "Animal models for implant biomaterial research in bone: a review.," *European cells & materials*, vol. 13, Jan. 2007, pp. 1–10.

[90] Smith, MC, and Sherman, DM, "Goat medicine," 2011.

[91] Mellado, M, Amaro, JL, and García, JE, "Factors affecting gestation length in goats and the effect of gestation period on kid survival,"*The Journal of ...*, 2000

[92] Kim, W. G., Cho, S. R., Sung, S. H., and Park, H. J., "A chronic heart failure model by coronary artery ligation in the goat," *The International journal of artificial organs*, vol. 26, Oct. 2003, pp. 929–34.

[93] McCoy, A. M., "Animal Models of Osteoarthritis: Comparisons and Key Considerations.," *Veterinary pathology*, vol. 52, Sep. 2015, pp. 803–18.

[94] Jülke, H., Mainil-Varlet, P., Jakob, R. P., Brehm, W., Schäfer, B., and Nesic, D., "The Role of Cells in Meniscal Guided Tissue Regeneration: A Proof of Concept Study in a Goat Model.," *Cartilage*, vol. 6, Jan. 2015, pp. 20–9.

[95] Bobyn, J. D., Little, D. G., Gray, R., and Schindeler, A., "Animal models of scoliosis.,"*Journal of orthopaedic research : official publication of the Orthopaedic Research Society*, vol. 33, Apr. 2015, pp. 458–67.

[96] Chen, W.-T. T., Zhang, P.-X. X., Xue, F., Yin, X.-F. F., Qi, C.-Y. Y., Ma, J., Chen, B., Yu, Y.-L. L., Deng, J.-X. X., and Jiang, B.-G. G., "Large animal models of human cauda equina injury and repair: evaluation of a novel goat model.," *Neural regeneration research*, vol. 10, Jan. 2015, pp. 60–4.

[97] Matute-Bello, G, and Frevert, CW, "Animal models of acute lung injury," *American Journal of ...*, 2008.

[98] Matute-Bello, G, Downey, G, and Moore, BB, "An official American Thoracic Society workshop report: features and measurements of experimental acute lung injury in animals,"*American Journal of …*, 2011.

[99] Lecuit, M, "Human listeriosis and animal models," *Microbes and infection*, 2007.

[100] Uzal, F. A., McClane, B. A., Cheung, J. K., Theoret, J., Garcia, J. P., Moore, R. J., and Rood, J. I., "Animal models to study the pathogenesis of human and animal Clostridium perfringens infections.," *Veterinary microbiology*, vol. 179, Aug. 2015, pp. 23–33.

[101] ADLER, "Origin of the Golden Hamster Cricetus auratus as a Laboratory Animal," *Nature*, vol. 162, 1948.

[102] "BIO BREEDERS INC," *BIO BREEDERS INC* Available: http://www.biobreeders.com/hamstermodels.html.

[103] Lossi, L., D'Angelo, L., Girolamo, P. De, and Merighi, A., "Anatomical features for an adequate choice of experimental animal model in biomedicine: II. Small laboratory rodents, rabbit, and pig.," *Annals of anatomy = Anatomischer Anzeiger : official organ of the Anatomische Gesellschaft*, Oct. 2015.

[104] "Hamsters: Biology, Care, and Disease Models" Available: http://netvet.wustl.edu/species/hamsters/hamstbio.txt.

[105] Gimenez-Conti, I. B., and Slaga, T. J., "The hamster cheek pouch carcinogenesis model.,"*Journal of cellular biochemistry. Supplement*, vol. 17F, Jan. 1993, pp. 83–90.

[106] Vairaktaris, E., Spyridonidou, S., Papakosta, V., Vylliotis, A., Lazaris, A., Perrea, D., Yapijakis, C., and Patsouris, E., "The hamster model of sequential oral oncogenesis.," *Oral oncology*, vol. 44, Apr. 2008, pp. 315–24.

[107] Sakamoto, A., "Electrical and ionic abnormalities in the heart of cardiomyopathic hamsters: in quest of a new paradigm for cardiac failure and lethal arrhythmia.,"*Molecular and cellular biochemistry*, vol. 259, Apr. 2004, pp. 183–7.

[108] Escobales, N., and Crespo, M. J. J., "Early pathophysiological alterations in experimental cardiomyopathy: the Syrian cardiomyopathic hamster.," *Puerto Rico health sciences journal*, vol. 27, Dec. 2008, pp. 307–14.

[109] Cheema, S., and Cornish, M., "Bio F1B hamster: a unique animal model with reduced lipoprotein lipase activity to investigate nutrient mediated regulation of lipoprotein metabolism," *Nutrition & Metabolism*, vol. 4, 2007, p. 27.

[110] Kawamoto, H., Ohyanagi, M., Nakamura, K., Yamamoto, J., and Iwasaki, T., "Increased levels of inhibitory G protein in myocardium with heart failure.," *Japanese circulation journal*, vol. 58, Dec. 1994, pp. 913–24.

[111] Roberts, A., and Subbarao, K., "Animal models for SARS.," *Advances in experimental medicine and biology*, vol. 581, Jan. 2006, pp. 463–71.

[112] Wahl-Jensen, V., Bollinger, L., Safronetz, D., Kok-Mercado, F. de, Scott, D. P., and Ebihara, H., "Use of the Syrian hamster as a new model of ebola virus disease and other viral hemorrhagic fevers.," *Viruses*, vol. 4, Dec. 2012, pp. 3754–84.

[113] Ebihara, H., Zivcec, M., Gardner, D., Falzarano, D., LaCasse, R., Rosenke, R., Long, D., Haddock, E., Fischer, E., Kawaoka, Y., and Feldmann, H., "A Syrian golden hamster model recapitulating ebola hemorrhagic fever," *The Journal of infectious diseases*, vol. 207, Jan. 2013, pp. 306–18.

[114] Wold, W. S., and Toth, K., "Chapter three--Syrian hamster as an animal model to study oncolytic adenoviruses and to evaluate the efficacy of antiviral compounds.," *Advances in cancer research*, vol. 115, Jan. 2012, pp. 69–92.

[115] Zivcec, M., Safronetz, D., Haddock, E., Feldmann, H., and Ebihara, H., "Validation of assays to monitor immune responses in the Syrian golden hamster (Mesocricetus auratus)," *Journal of Immunological Methods*, vol. 368, 2011.

[116] Tchitchek, N., Safronetz, D., Rasmussen, A., Martens, C., Virtaneva, K., Porcella, S., Feldmann, H., Ebihara, H., and Katze, M., "Sequencing, Annotation and Analysis of the Syrian Hamster (Mesocricetus auratus) Transcriptome," *PLoS ONE*, vol. 9, 2014.

[117] "Approved Sequencing Targets Archive," Approved Sequencing Targets Archive Available: http://www.genome.gov/10002154.

[118] Fan, Z., Li, W., Lee, S. R., Meng, Q., Shi, B., Bunch, T. D., White, K. L., Kong, I.-K. K., and Wang, Z., "Efficient gene targeting in golden Syrian hamsters by the CRISPR/Cas9 system.," *PloS one*, vol. 9, Jan. 2014, p. e109755.

[119] Toth, K., Lee, S. R., Ying, B., Spencer, J. F., Tollefson, A. E., Sagartz, J. E., Kong, I.-K. K., Wang, Z., and Wold, W. S., "STAT2 Knockout Syrian Hamsters Support Enhanced Replication and Pathogenicity of Human Adenovirus, Revealing an Important Role of Type I Interferon Response in Viral Control.,"*PLoS pathogens*, vol. 11, Aug. 2015, p. e1005084.

[120] Riele, T. H., and Maandag, ER, "Highly efficient gene targeting in embryonic stem cells through homologous recombination with isogenic DNA constructs," *Proceedings of the …*, 1992.

[121] Yanez, RJ, and Porter, AC, "Therapeutic gene targeting.," *Gene therapy*, vol. 5, 1998, pp. 149–159.

[122] Smithies, O., Gregg, R. G., Boggs, S. S., Koralewski, M. A., and Kucherlapati, R. S., "Insertion of DNA sequences into the human chromosomal beta-globin locus by homologous recombination.," *Nature*, vol. 317, Jan. 1985, pp. 230–4.

[123] Thomas, K. R., Folger, K. R., and Capecchi, M. R., "High frequency targeting of genes to specific sites in the mammalian genome.," *Cell*, vol. 44, Feb. 1986, pp. 419–28.

[124] Mansour, S. L., Thomas, K. R., and Capecchi, M. R., "Disruption of the proto-oncogene int-2 in mouse embryo-derived stem cells: a general strategy for targeting mutations to non-selectable genes.," *Nature*, vol. 336, Nov. 1988, pp. 348–52.

[125] Wei, C., Liu, J., Yu, Z., Zhang, B., Gao, G., and Jiao, R., "TALEN or Cas9 – Rapid, Efficient and Specific Choices for Genome Modifications," *Journal of Genetics and Genomics*, vol. 40, 2013.

[126] Sakuma, T., and Woltjen, K., "Nuclease-mediated genome editing: At the front-line of functional genomics technology," *Development, Growth & Differentiation*, vol. 56, 2014, pp. 2–13.

[127] Cong, L., Ran, F. A., Cox, D., Lin, S., Barretto, R., Habib, N., Hsu, P. D., Wu, X., Jiang, W., Marraffini, L. A., and Zhang, F., "Multiplex genome engineering using CRISPR/Cas systems.," *Science (New York, N.Y.)*, vol. 339, Feb. 2013, pp. 819–23.

[128] Doudna, JA, and Charpentier, E, "The new frontier of genome engineering with CRISPR-Cas9," *Science*, 2014.

[129] Ni, W., Qiao, J., Hu, S., Zhao, X., Regouski, M., Yang, M., Polejaeva, I. A., and Chen, C., "Efficient gene knockout in goats using CRISPR/Cas9 system.," *PloS one*, vol. 9, Jan. 2014, p. e106718.

[130] Li, M., Suzuki, K., Kim, N., Liu, G.-H., and Belmonte, J., "A Cut above the Rest: Targeted Genome Editing Technologies in Human Pluripotent Stem Cells," *Journal of Biological Chemistry*, vol. 289, 2014, pp. 4594–4599.

[131] Cencic, R., Miura, H., Malina, A., Robert, F., Ethier, S., Schmeing, T. M., Dostie, J., and Pelletier, J., "Protospacer adjacent motif (PAM)-distal sequences engage CRISPR Cas9 DNA target cleavage.," *PloS one*, vol. 9, Jan. 2014, p. e109213.

[132] Sternberg, S. H., Redding, S., Jinek, M., Greene, E. C., and Doudna, J. A., "DNA interrogation by the CRISPR RNA-guided endonuclease Cas9.," *Nature*, vol. 507, Mar. 2014, pp. 62–7.

[133] Zhou, X., Xin, J., Fan, N., Zou, Q., Huang, J., Ouyang, Z., Zhao, Y., Zhao, B., Liu, Z., Lai, S., Yi, X., Guo, L., Esteban, M. A., Zeng, Y., Yang, H., and Lai, L., "Generation of CRISPR/Cas9-mediated gene-targeted pigs via somatic cell nuclear transfer.," *Cellular and molecular life sciences : CMLS*, vol. 72, Mar. 2015, pp. 1175–84.

[134] Choi, W., Yum, S., Lee, S., Lee, W., Lee, J., Kim, S., Koo, O., Lee, B., and Jang, G., "Disruption of exogenous eGFP gene using RNA-guided endonuclease in bovine transgenic somatic cells.," *Zygote (Cambridge, England)*, vol. 23, Dec. 2015, pp. 916–23.

[135] Fujii, W., Kawasaki, K., Sugiura, K., and Naito, K., "Efficient generation of large-scale genome-modified mice using gRNA and CAS9 endonuclease," *Nucleic Acids Research*, vol. 41, 2013, pp. e187–e187.

[136] Wang, H., Yang, H., Shivalila, C., Dawlaty, M., Cheng, A., Zhang, F., and Jaenisch, R., "One-Step Generation of Mice Carrying Mutations in Multiple Genes by CRISPR/Cas-Mediated Genome Engineering," *Cell*, vol. 153, 2013.

[137] Harms, D. W., Quadros, R. M., Seruggia, D., Ohtsuka, M., Takahashi, G., Montoliu, L., and Gurumurthy, C. B., "Mouse Genome Editing Using the CRISPR/Cas System.," *Current protocols in human genetics / editorial board, Jonathan L. Haines ... [et al.]*, vol. 83, Jan. 2014, pp. 15.7.1–15.7.27.

[138] Crispo, M., Mulet, A. P., Tesson, L., Barrera, N., Cuadro, F., Santos-Neto, P. C. dos, Nguyen, T. H., Crénéguy, A., Brusselle, L., Anegón, I., and Menchaca, A., "Efficient Generation of Myostatin Knock-Out Sheep Using CRISPR/Cas9 Technology and Microinjection into Zygotes.," *PloS one*, vol. 10, Jan. 2015, p. e0136690.

[139] Wang, X, Yu, H, Lei, A, Zhou, J, Zeng, W, and Zhu, H, "Generation of gene-modified goats targeting MSTN and FGF5 via zygote injection of CRISPR/Cas9 system," *Scientific ...*, 2015.

[140] Zhou, X, Wang, L, Du, Y, Xie, F, Li, L, Liu, Y, and Liu, C, "Efficient Generation of Gene‑Modified Pigs Harboring Precise Orthologous Human Mutation via CRISPR/Cas9‑Induced Homology‑Directed Repair in Zygotes,"*Human ...*, 2015.

[141] Chow, Y.-H., Plumb, J., Wen, Y., Steer, B. M., Lu, Z., Buchwald, M., and Hu, J., "Targeting transgene expression to airway epithelia and submucosal glands, prominent sites of human CFTR expression," *Molecular Therapy*, vol. 2, 2000, pp. 359–367.

[142] Ibrahimi, A., Velde, G., Reumers, V., Toelen, J., Thiry, I., Vandeputte, C., Vets, S., Deroose, C., Bormans, G., Baekelandt, V., Debyser, Z., and Gijsbers, R., "Highly Efficient Multicistronic Lentiviral Vectors with Peptide 2A Sequences," *Human Gene Therapy*, vol. 20, 2009.